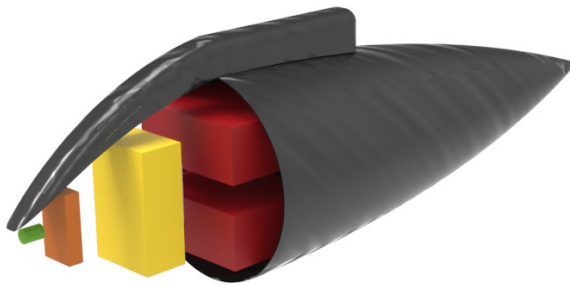


# Thermodynamic Well to Wheel analysis of using compressed SNG derived from biomass for an SOFC-GT powered UAV



by  
Hardik Joshi

For the degree of Master of Science in Sustainable Energy Technology at  
Delft University of Technology

Supervisors:

Dr. P.V. Aravind  
Ir. T. Woudstra  
Álvaro Fernandes

Faculty of Mechanical, Maritime and Materials Engineering  
Master Sustainable Energy Technology  
Department of Process and Energy  
Delft University of Technology  
Report No. 2653



This report is developed under the supervision of:  
Dr. P.V. Aravind

The examination committee consists of  
Prof.dr.ir. J.H.A. Kiel Chairman  
Dr.ir. H.J. van der Kooi  
Dr. P.V. Aravind  
Ir. Theo Woudstra  
Dr. A.A. Eftekhari  
Álvaro Fernandes



# Acknowledgements

Distraction and focus, commotion and calm, delight and disappointment. The author does not feel the need to use more words than these to describe the past few months. An individual can only take so much before he asks for help. But fortunately for the author, he never had to look very far. He would like to extend his heartfelt gratitude to his daily supervisor Álvaro Fernandes for his ceaseless support throughout the course of this learning adventure. Not to forget Theo Woudstra for his refined views on thermodynamics and unmatched insight into operation of Cycle-Tempo. Finally, the author thanks P.V. Aravind for arranging an unconventional ending to this work despite his extremely busy schedule.

In the background, the author cannot overstate the contribution of friends and family. For they were always around and this assurance enabled him to take far greater risks and reach far greater heights. He would like to specially acknowledge the expert help provided by *Anil Kumar Ananda*, *Davide Zanon* and *Johnathan Hoogvliet* in certain critical areas of the project. Also, the author realizes that this will not be the last time he will encounter such situations and hope to continue to deserve the help and support of his dear ones.

*She said, "Hey, bossa nova baby keep on workin' for this ain't no time to quit"*

From *Bossa Nova Baby* by Elvis



# Abstract

Unmanned aerial vehicles (UAV) for science missions are becoming increasingly popular in the present context. Science missions require high altitude operation and long endurance (HALE). With rising awareness of climate change phenomenon it becomes imperative to look into more efficient and more sustainable means of powering these missions. A 'well-to-wheel' study is a comprehensive way of comparing different operations for powering a vehicle. For this study, the HALE UAV is powered by a solid oxide fuel cell and gas turbine (SOFC-GT) hybrid. The HALE UAV design is based on concept that has been developed before by NASA. It is also essential that a suitable fuel is selected for powering the hybrid system. Previous studies which were based on liquid hydrogen ( $LH_2$ ) concluded that liquefaction of hydrogen as an avenue for major exergy losses. For the current study, use of compressed synthetic natural gas (SNG) is analysed. Exergy analysis is carried out for fuel production and the hybrid system operation at cruise altitude. To begin with, syngas is synthesised from woody biomass through gasification. The syngas is then converted into SNG and compressed for storage. This SNG is utilised in the SOFC-GT hybrid. Design calculations are made for the take-off stage. Effect of pressure variation is studied to get the optimum system size. Then the performance of the system is analysed in the cruising stage to estimate the endurance of the flight. Exergy efficiency analysis and mission endurance calculations are made for the system during cruising conditions as a means to evaluate the system performance. The effect of position of air preheater is studied in two different configurations. The exergy efficiency for compressed SNG synthesis is 59.7% and the SOFC-GT operation at cruise is 69.6% efficient. A total 'well-to-wheel' efficiency of 41.6 % is attained. Based on the results of the analysis carried out thus far, the mass for the system components is estimated. Volumetric estimates are also made and the system is fitted in the nacelle volume as defined in NASA concept. The results are eventually compared to the system working on  $LH_2$ . The results from compressed SNG study show that specific energy density of the fuel is important. The mass estimates show that the infrastructure required to carry the SNG fuel reduces the specific energy of the fuel. liquid fuels such as methanol should be analysed as another option.

---

# Contents

Nomenclature List	
Problem Introduction	15
Technical Review	17
Thermodynamics	22
System Description	24
Results and discussions	29
Conclusions	37
Appendices	



---

## List of Tables

Table 1	Different types of fuel cell technologies (LARMINIE, 2003)	19
Table 2	Birch wood composition (Phyllis, 2000)	24
Table 3	Component specifications for different reactor blocks in ASPEN	25
Table 4	Process steam generated in the gasification system for different reactors.	25
Table 5	Input parameters for SOFC-GT design condition simulation	26
Table 6	Mission requirements for the HALE UAV	27
Table 7	Irreversibilities in gasification plant for the production of compressed SNG	29
Table 8	Sensitivity analysis of SOFC-GT system with different operating pressures	30
Table 9	Exergetic Efficiency(%) and Area(m <sup>2</sup> ) of SOFC-GT system operation in different conditions. A and B refer to two configurations of air preheater.	31
Table 10	A comparison of Performance parameters for SOFC-GT hybrid system during off-design conditions.	31
Table 11	Mass of different components in th propulsion system	34
Table 12	Component sizes for the nacelle assembly. W = width, L= length, D= diameter, H=height.	35
Table 13	Comparison of performance paramters for the liquid hydrogen and compressed SNG systems for powering the HALE UAV.	35

---

## List of Figures

Figure 1	Specific energy vs energy density for various fuels(USEIA, 2013).	16
Figure 2	Breakdown schem of gasification process. (Adapted from (HIGMAN ET AL, 30))	17
Figure 3	Solid oxide fuel cell operating principle (SOURCE: HUISMANS ET AL., 1998)	18
Figure 4	Tubular SOFC design (SINGHAL, 2000)	19
Figure 5	Steps for calculating the chemical exergy of a molecule	22
Figure 6	Scheme for production of Syngas	24
Figure 7	Adiabatic fixed bed methanation reactor scheme. (Heyne et. al, 2006)	25
Figure 8	Scheme of SOFC-GT hybrid operation	26
Figure 9	Breakdown of irreversibilities durng production of compressed SNG in the gasification plant.	29
Figure 10	Grassman diagram depicting exergy flows in compressed SNG production	30
Figure 11	Plot showing the results of sensitivity analysis. Efficiency is plotted against the SOFC operating pressure.	31
Figure 12	Irreversibilities in different components during off design operation of the hybrid system. In the legend, C stands for cruise, (1.5/5) shows the operating pressure during take off and the configuration of air preheater (A/B).	32
Figure 13	Grassman diagram for the SOFC-GT system operating in off-design conditions (in cruise reference environment) with air preheater configuration B.	33
Figure 14	Specific power of turbochargers plotted against the net power produced (Capstone), (Turbec), (Elliot).	34
Figure 15	Power train for the SOFC-GT system for powering the UAV.	34
Figure 16	Assembly of components in the nacelle. Electric motor is shown in green, inverter in orange, SOFCstack in yellow, turbochargers in red and CNG tanks in blue. Heat exchanger is in purple.	35

## Nomenclature List

Abbreviations

<b>Short hand</b>	<b>Full form</b>
CGO	Gadolinium doped ceria
ch	chemical
CNDNS	Condensation
CO2SEP	CO <sub>2</sub> separation
CompStorage	Compressor storage
FICFB	Fast internally circulated fluidised bed
GHG	Greenhouse gases
GSF	Gasifier
GT	Gas turbine
HALE	High altitude long endurance vehicle
HTS	High temperature Shift reaction
MTHN	Methanation reactor
LH <sub>2</sub>	Liquid Hydrogen
PEM	Proton exchange membrane
ph	physical
SNG	synthetic natural gas
SOFC	Solid oxide fuel cell
TET	Turbine exit temperature
TIT	Turbine inlet temperature
TTW	Tank to wheel
UAV	Unmanned aerial vehicle
WTT	well to tank
YSZ	Yttria stabilized Zirconia

Symbols

<b>Variable</b>	<b>meaning</b>	<b>units</b>
$\varepsilon$	Specific exergy	kJ/kg
$g$	acceleration due to gravity	m/s <sup>2</sup>
$\bar{g}$	Gibbs free energy per mole	J/mol
$\bar{h}$	Specific enthalpy	J/kg
$h$	Enthalpy per mole	J/mol
$m$	Mass	kg
$v$	Number of mole	
$\dot{P}$	Power delivered by the system	J/s
$\dot{Q}$	rate of flow of heat into the system	J/s
$\bar{R}$	Universal gas constant	J/mol.K
$\bar{s}$	Entropy per mole	J/mol.K
$S$	Entropy	J/K
$T$	Temperature	K
$U$	internal energy	J
$\dot{v}$	centre of mass velocity	m/s
$\dot{W}$	rate of work done by the system	J/s
$x$	Mole fraction	
$z$	Height	m

<b>Variable</b>	<b>meaning</b>
0	Standard conditions at sea level
C	compressor
gen	generated
in	inflow
out	outflow
k	index variable
sat	Saturation
T	Turbine

*Naming convention for the SOFC-GT model*

<b>ID</b>	<b>Description</b>
Comb	Combustor
Comp 108	Anode recirculation compressor
Comp 202	1st stage compressor
Comp 205	2nd stage compressor
Comp 210	Cathode recirculation compressor
FC	Fuel Cell
Gen	Generator
GT1	1st stage gas turbine
GT2	2nd stage gas turbine
HEX 206-207	Cathode recirculation mixer
HEX103	Fuel preheater
HEX205	Air preheater
Node104	Anode recirculation mixing node.
Stack	Stack
XP valve	Fuel expansion valve



# Problem Introduction

Transportation sector is one of the major consumers of energy. Prior to development of first commercial steam turbines by James Watt in 1776, navigating land and water was a laborious task and flight was still a dream. Steam engines and locomotives gave a new outlet for the human urge to move. Since then various designs of engines for land, sea and air have been developed. In midst of all these developments, human consciousness has grown over subjects of equivocal misuse of the planet's resources for fueling human ambitions. A call for sustainable practices in all areas of human endeavor has already been made and transportation is not left untouched. Estimates have been made to determine the share of damage caused by transportation to the health of the planetary ecosystem. Reports estimate that transportation sector contributes 13.1% globally to greenhouse gas (GHG) emissions and 23% of energy related CO<sub>2</sub> emissions. Also, it is noteworthy that GHG emissions from transport has grown at a faster rate than any other energy using sector. Air transportation is responsible for 11% of total energy used in the transportation sector (IPCC, 2007). An interesting opportunity emerges to make air transport more energy efficient to reduce GHG emissions. Biomass derived fuels can have a neutral CO<sub>2</sub> fuel cycle (Gustavsson et al., 1995) and carbon capture and storage systems can even lead to CO<sub>2</sub> savings.

## *High Altitude Long endurance unmanned aerial vehicles*

In order to reduce system redundancies and human risks associated with flights, unmanned aerial vehicles are increasingly being deployed. Unmanned aerial vehicles (UAV) or drones, as they are called in popular culture, were developed to serve military missions in early years. Since then, applications have matured and broken into more mainstream areas. Study of hurricanes, reconnaissance missions, package delivery and wildlife protection are gaining interest. This study is focused entirely on High altitude long endurance (HALE) UAVs that fly at an altitude of 21 km and have a desirable mission time of 1 week. NASA has undertaken various studies for powering HALE UAVs with alternate fuels (Nickol et al., 2007). Mission requirements were set and different fuel options were considered for the powering the UAV. It has to be mentioned that Proton exchange membrane (PEM) fuel cells were considered as a concept for the UAV. The fuel used for this application was liquid hydrogen. Other models have also been proposed in the study which include regenerative fuel cells in combination with solar cells, solar cells and batteries and combustion technologies such as internal combustion engine and

gas turbines, both consuming liquid hydrogen. Solid oxide fuel cell based technologies have also been considered in combination with gas turbines (Aguilar, P. et al., 2008).

## *'Well-to-Wheel' / Thermodynamic Analysis*

With the increasing number of policy constraints regarding environmental impact of human activities, it is critical that a holistic approach is developed to assess their impact (Wara et al., 2008), (Parry et al., 2009). A good example would be a fuel cell vehicle that works on hydrogen. It will be very easy to point that such a vehicle is not emitting any carbon dioxide (CO<sub>2</sub>) and can so be labeled as a zero-emissions vehicle. However, when the production of hydrogen is brought into the picture, there is a dramatic change. Production of hydrogen itself can result in large CO<sub>2</sub> emissions depending on the type of technology employed for the production process (Koroneos et al., 2004). This certainly establishes a base for studying the entire life cycle of a fuel option from its source to the point of consumption. Such studies, documented as 'Well-to-Wheels' studies, have been undertaken in order to determine in the most complete form, suitability of a fuel for a given environmentally friendly application. Strictly confining the study to transportation options, there are studies conducted for the European region specifically considering different drive train options and fuels (Edwards, 2014). These studies are usually broken down into Well to Tank (WTT) and Tank to Wheel (TTW) analysis and deal in inland transportation options. They provide insights about most energy intensive steps in the process. It should be pointed out that a 'well-to-wheel' study is a comprehensive work, and could include as many as 88 fuel pathways and multiple power trains for a given application area (LBST, 2003)

## *Current Study*

On the subject of this work, there are not many studies available that make use of 'well-to-wheels' analysis for a UAV. The present study on using compressed SNG is motivated from a previous study that considered liquid H<sub>2</sub> as a fuel for the SOFC-GT Hybrid system (Fernandes et al., 2014). In order to attain high specific energy, H<sub>2</sub> is liquified. But it was reported that the major exergy losses were encountered during the liquefaction process and therefore a step towards increasing the exergetic efficiency would be the removal of this step during fuel production. SNG does not require liquefaction and can be transported in compressed form. Also, it has a higher volumetric energy

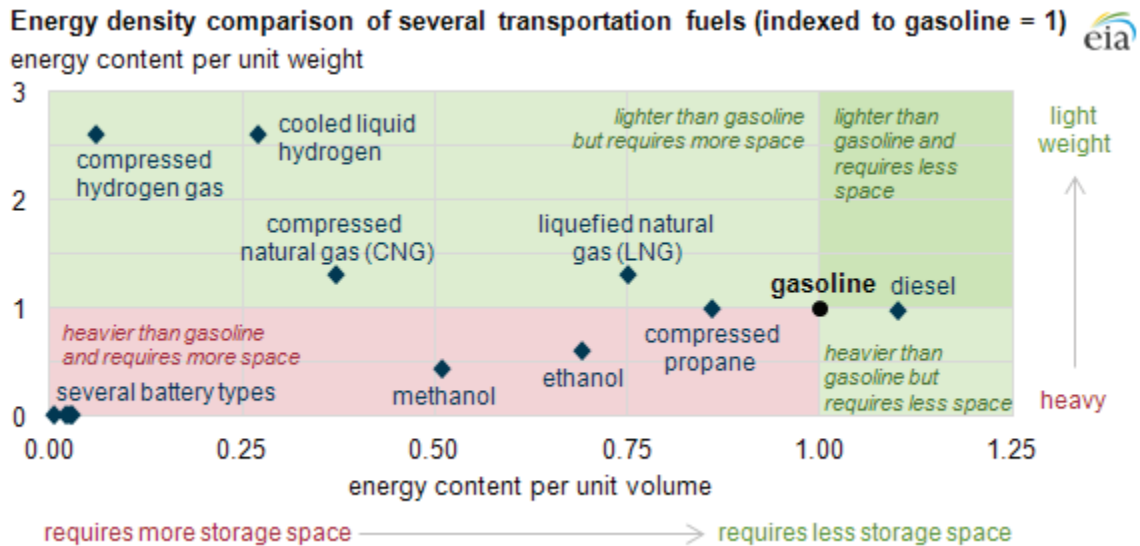


Figure 1 Specific energy vs energy density for various fuels (USEIA, 2013).

density. However, the specific energy of the fuel goes down. This can be seen clearly in Figure 1. In the current study compressed SNG is utilised for powering the hybrid SOFC-GT system.

References

Aguiar, P., D. J. L. Brett, and N. P. Brandon. "Solid oxide fuel cell/gas turbine hybrid system analysis for high-altitude long-endurance unmanned aerial vehicles." *International Journal of Hydrogen Energy* 33.23 (2008): 7214-7223.

Edwards, Robert; et al., WELL-TO-WHEELS ANALYSIS OF FUTURE AUTOMOTIVE FUELS AND POWERTRAINS IN THE EUROPEAN CONTEXT. Tech. N.p.: Joint Research Centre, the European Commission, 2014. Web. 29 Sept. 2014. <[http://iet.jrc.ec.europa.eu/about-jec/sites/iet.jrc.ec.europa.eu/about-jec/files/documents/wtw\\_report\\_v4a\\_march\\_2014\\_final\\_333\\_rev\\_140408.pdf](http://iet.jrc.ec.europa.eu/about-jec/sites/iet.jrc.ec.europa.eu/about-jec/files/documents/wtw_report_v4a_march_2014_final_333_rev_140408.pdf)>.

Fernandes, A et al. "Thermodynamic analysis of use of biomass-derived liquid hydrogen for a solid oxide fuel cell-gas turbine-powered aircraft." 2014. TU Delft.

Gustavsson, Leif, et al. "Reducing CO<sub>2</sub> emissions by substituting biomass for fossil fuels." *Energy* 20.11 (1995): 1097-1113.

Intergovernmental Panel on Climate Change. *Climate Change 2007 - Mitigation of Climate Change: Working Group III contribution to the Fourth Assessment Report*

of the IPCC. Cambridge: Cambridge University Press, 2007. Ebook Library. Web. 29 Sep. 2014.

Koroneos, C., et al. "Life cycle assessment of hydrogen fuel production processes." *International Journal of Hydrogen Energy* 29.14 (2004): 1443-1450.

LBST, "Results of the GM WtW study", March 2003. Web. 29 Sept. 2014 <<http://heliev.gr/?wpdmact=process&did=MjAuaG90bGluaw.>>

Nickol, Craig L., et al. "High altitude long endurance UAV analysis of alternatives and technology requirements development." (2007).

Parry, Martin, Jason Lowe, and Clair Hanson. "Overshoot, adapt and recover." *Nature* 458.7242 (2009): 1102-1103.

"U.S. Energy Information Administration - EIA - Independent Statistics and Analysis." *Few Transportation Fuels Surpass the Energy Densities of Gasoline and Diesel*. EIA, 14 Feb. 2013. Web. 19 Oct. 2014.

Wara, Michael W., and David G. Victor. "A realistic policy on international carbon offsets." *Program on Energy and Sustainable Development Working Paper* 74 (2008): 1-24.

# Technical Review

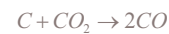
## Gasification of Biomass and SNG production

Power production is an important sector for any economy in the world. Traditionally the power production plants rely heavily on thermal breakdown of fossils and other hydrocarbon sources. Along with the heat that is released in the process which helps in producing electricity, carbon dioxide (CO<sub>2</sub>) is also released as a byproduct. With the advent of supply chain mapping and the hunt for CO<sub>2</sub> emission reducing strategies, these plants have been identified as a major CO<sub>2</sub> capture opportunity. The energy density of a fuel is often measured in terms of its Carbon to Hydrogen ratio(C-H) and this density is improved by either adding more hydrogen atom(s) per atom of carbon or by removing more carbon atom(s) per atom of Hydrogen. In short, decreasing the C-H ratio in the molecular composition of a fuel increases its energy density. In light of these facts, gasification becomes very relevant.

four sub processes. Figure 2 shows these processes in a sequence.

The fuel is first dried and water is removed as steam. Thereafter, the volatiles are removed from fuel. Devolatilization can occur in a range of temperatures and is dependent on the rate of heating. With slow heating rates this process can start at 350 °C and with faster heating rates, it can occur along with other processes at 800 °C. No oxygen is required for this process. Next process involves the combustion of the released volatiles which produces syngas mainly consisting of CO, CO<sub>2</sub>, H<sub>2</sub>, CH<sub>4</sub>. Following reactions are considered to be taking place (Higman et al., 10):

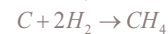
The Boudard reaction,



The water gas reaction,



The methanation reaction,



and the combustion reactions,

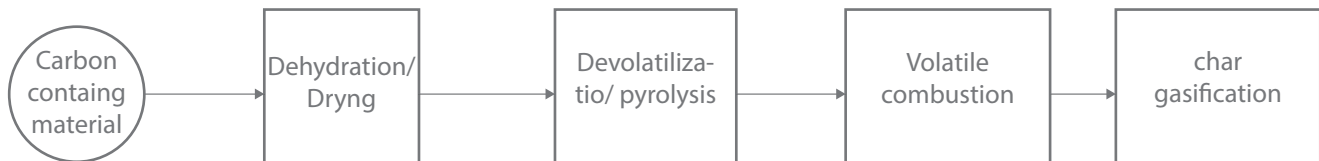
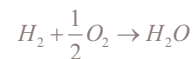
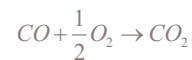
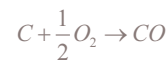


Figure 2 Breakdown schem of gasification process. (Adapted from (HIGMAN ET AL, 30))

Not only does it provide the opportunity to improve the energy density, it makes it possible to generate different fuels like methane and methanol which are excellent for storage. And not to forget, the opportunity to restrict CO<sub>2</sub> emissions at source is very welcome. Gasification is a complex process that involves various sub processes and chemical reactions that lead to a variety of intermediate species. These species are critical in determining the performance and yield of the gasification products. The study of these species and the chemical reactions that they partake in is an important area of research for gasification technologies. On a superficial level, the gasification process can largely be broken down into

### Feedstock Analysis

Various types of materials can be used as feedstock for gasification. Ranging from virgin wood to coal and even waste sludge, they differ in elemental composition. These compositions can be analysed by conducting proximate analysis and ultimate analysis. Proximate analysis determines moisture, volatile matter, fixed carbon and ash in the feedstock. Through ultimate analysis, carbon, hydrogen, oxygen, sulphur and nitrogen percentages are determined in the feedstock.

Based on the choice of feedstock, gasification technique is highly variable. Reportedly, biomass ash consists mainly of salts like potassium, calcium, phosphorus, magnesium, iron and silicon (Higman et al., 68). As a result the ash softening temperatures are very low. This restricts the temperature conditions inside the

gasification reactor.

### Choice of Gasifier

There are three types of gasifiers: Fixed bed gasifier, Fluidised bed gasifier and entrained flow gasifier. For the current study, Fluidised bed operation is most suitable because it operates below the ash softening temperature of the biomass. However, this also has a bearing on the carbon conversion rates. Low temperature operation limits the carbon conversion efficiency. One of the objectives in the current study is to produce synthetic natural gas (SNG) from biomass. The gasification of biomass results in formation of syngas (a mixture of CO, CO<sub>2</sub>, CH<sub>4</sub>, H<sub>2</sub> and other impurities in low concentrations like H<sub>2</sub>S, HCl and NH<sub>3</sub>). There are various constraints when choosing the right gasification process for a desired outlet composition. The operating temperature and pressure, the type of gasifier and the composition of the output gas are among the major criteria for making such decisions.

A study was conducted to compare the efficiency of conversion of woody biomass to SNG for three different types of gasification processes (van der Meijden et al., 2010). Entrained flow, circulating fluidized bed and allothermal gasification techniques were studied. It was concluded that allothermal gasifiers have the best overall efficiency for conversion of wood to SNG. Further study was conducted on the best practices for achieving high exergetic efficiencies in use of allothermal gasification techniques for production of SNG (Vitasari et al., 2011). It should be noted that under these studies methanation of syngas was investigated as well. The methanation process was completed by following the ICI (Imperial Chemical Industries). In this study, major exergy losses were reported in the gasification, methanation and SNG conditioning section. Reportedly, there is some leakage of methane during SNG conditioning. Recovery of this lost methane has also been suggested (Duret et al, 2005). This provides a strong case for use of allothermal gasification strategy for high exergy efficiency for conversion of woody biomass to SNG. The gasifier in the models thus developed uses a fast internal circulating fluidized bed (FICFB) gasification reactor.

### Fuel cells: Solid oxide fuel cells.

Fuel cells are simple devices that convert the chemical energy stored in molecules into electrical energy. Figure 3 below helps in conversion.

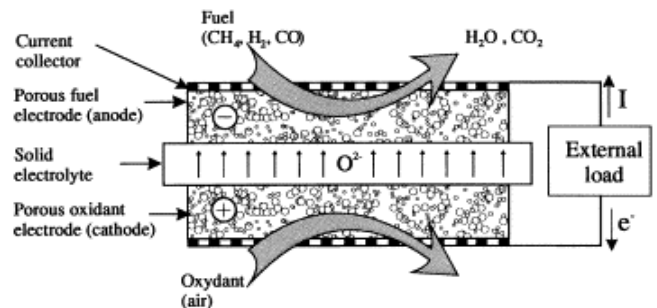
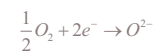
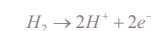


Figure 3 Solid oxide fuel cell operating principle (SOURCE: HUISMANS ET AL., 1998)

The cell consists of two layers of electrodes enclosing a layer of electrolyte. The fuel (gas phase) is fed to the anode and an oxidant (usually air/ oxygen) is fed to the cathode. The fuel molecule splits electrochemically releasing ions and electrons. These electrons travel through an external circuit and thereby give rise to an electric current. The electrons upon reaching the opposite electrode reduce the oxidant. The electrolyte helps in conducting mobile ionic species between the electrodes and thereby completing the cell reaction. A sample half cell reaction is shown below:



The path of this conversion process is electrochemical rather than thermochemical. Thermochemical processes are characterised by high exergy destruction rates. Energy as opposed to exergy is conserved in all processes and this is evident very prominently in thermochemical processes. The heat accompanying a thermochemical process is less useful and is described as having lesser exergy. Electrochemical processes on the other hand have significantly lesser problems of this nature. Fuel cells themselves can be categorised into several types. The fuel cell technologies have been growing leaps and bounds since their first much publicised use in the Apollo mission in 1954. Alkaline fuel cells were used for this mission. Since then various technologies have come to the fore and have gained much popularity in the scientific community. With the availability of a range of operating temperatures, and a range of fuels that can be utilised in fuel cells, the usage varies from case to case. Table 1 above provides an overview of types of fuel cells.



Fuel Cell Types	Electrodes		Electrolytes	Operating Temperatures
	Cathode	Anode		
Alkaline FC	C supported catalyst mixed with PTFE	C supported catalyst mixed with PTFE	NaOH/KOH solution	50-200 °C
PEMFC	Pt/ porous C	Pt/ porous C	Nafion	30-100 °C
PAFC	C supported Pt black bonded to PTFE	C supported Pt black bonded to PTFE	H <sub>3</sub> PO <sub>4</sub>	220 °C
DMFC	C supported Pt/Ru catalyst	C supported Pt catalyst		20-90 °C
MCFC	Lithiated NiO	Porous Ni-Cr/Ni-Al alloy	$\alpha, \beta$ LiAlO <sub>2</sub> supported Li-K/Li-Na alloy	650 °C
SOFC	Strontium doped Lanthanum manganite (LSM)	Zirconia cermet ( with Ni as the metal)	Yttria-stabilized Zirconia (YSZ)	500-1000 °C

Table 1 Different types of fuel cell technologies (LARMINIE, 2003)

#### SOFC Design - Cell structure: Electrodes/Electrolyte, Packaging

An important performance parameter for SOFC performance is its power density. The arrangement of multiple cells results in a stack. These stacks can be arranged in different ways so as to minimize the volume they occupy. Certain application areas, especially mobile power systems, require large power densities. Hence it becomes imperative for the stack designer to attain maximum power density. SOFCs are being made predominantly either in planar or tubular geometries. A tubular SOFC design is shown in Figure 4. These geometries enable integration of cells to form a stack thus allowing for uniform fuel and air distribution. This helps in providing a much needed thermal and mechanical strength.

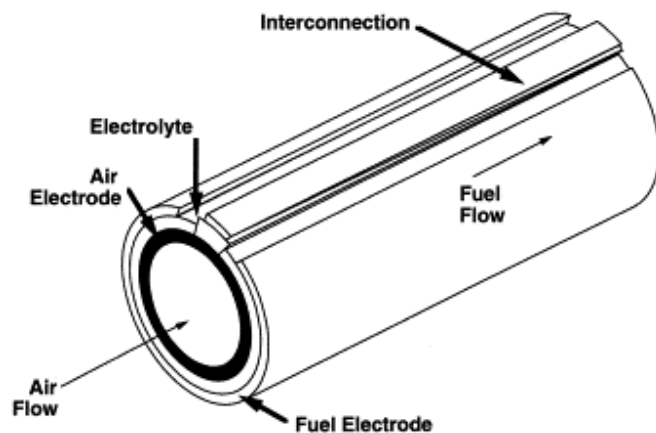


Figure 4 Tubular SOFC design (SINGHAL, 2000)

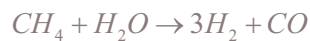
The anode and cathode layers are deposited with techniques such as Electro vapour Deposition (EVD) and plasma enhanced vapour deposition (PEVD). The basic technology uses ceramic materials to add the much needed thermal insulation for safe operation. Traditionally, either the electrolyte or one of the electrode layers is made much thicker than the rest, thereby providing the mechanical support for the entire cell. With improvements in material science and manufacturing capabilities, it has become possible to deposit metal-supported cells containing porous metallic layers to provide the mechanical stability. These materials have higher resistance to thermal stress and mechanical shocks.

Cathode is designed to be of sufficient porosity and is made usually from strontium doped Lanthanum Manganite (LSM) or lanthanum strontium cobalt iron oxide (LSCF) as the base material. It should be pointed out that cathodes with adequate porosity are essential for improved current densities. For anodes the most common material is a Nickel Zirconia cermet. However, this anode shows deactivation with carbon deposition and low tolerance for sulphur. For direct utilisation of hydrocarbons this can be problematic. Alternate materials such as Strontium doped Lanthanum Chromium Manganite (LSCM) and Strontium doped Magnesium Molybdenum oxide (SMM) have been successfully deployed (Yang et al., 2012). The most commonly used electrolyte is Yttria stabilised Zirconia that becomes oxide ion conducting at temperatures above 800 °C .

Gadolinium doped ceria (CGO) is also an option for low temperature utilisation (above 500 °C) as conductivity of CGO is higher than YSZ (Tucker et al., 2010). However, for low temperature operation external fuel reforming is required.

#### *Fuel Reforming in the fuel cell*

As already emphasized before, SOFCs offer tremendous flexibility in terms of types of fuels that can be utilized for operation. The fuel cell system can ingest a hydrocarbon molecule, for example, methane and owing to its high operation temperature, thermo-chemically convert methane into hydrogen and carbon monoxide. Such a system is called a direct hydrocarbon system. In the simplest sense, this conversion is represented in the following equation:



This reaction is called as the steam methane reformation (SMR) reaction. There are two options for carrying out the hydrocarbon reformation. This reaction can be carried out externally or internally. To complicate it further, internal reforming can be completed in two ways- directly and indirectly. In direct internal reforming there is no need to employ an additional reformer reactor. The SMR reaction takes place inside the fuel cell, making use of the heat and steam available within the cell. By avoiding an external reformer it reduces the space constraints of the system. Very obviously, mobile applications can benefit significantly from this.

Indirect internal reforming reaction consists of a closely mounted assembly of SOFC stack and reformer reactor which are placed in close contact with each other to make use of the heat generated within the fuel cell. It is possible to reform the fuel in the storage before it is fed to the SOFC. Such systems make use of recuperators to generate the required steam in a heat recovery steam generator.

SMR is favoured with high temperature, steam and catalysts. However, this reaction is a congruence of several sub-reactions yielding a range of intermediate products including CO<sub>2</sub> and C. The formation of C, referred to as coking, is a significant problem in direct hydrocarbon fuel cells. It poisons the catalyst surface and therefore reduces the effectiveness of other reactions taking place on the electrode- the most important of which is the electrochemical oxidation of hydrogen.

#### *Hybrid operations with Gas Turbines*

The nature of operation of SOFC makes it possible to

use the exhaust stream in multiple ways. This exhaust is a gas mixture at a high temperature (800-1000 °C) and these are very favourable conditions for a gas turbine feed. The ability to use it in combination for a steam generator/turbine and/or a gas turbine (GT) has been known since many years. However, the present study does not warrant the use of steam and therefore, the GT operation is much more interesting. The first SOFC/GT pressurised hybrid plant of 200 kWe capacity was demonstrated by Siemens Westinghouse in 2000 (Larminie et al, 2003), (Veyo et al., 2003). Since then, many pressurised hybrid SOFC/GT systems have been tested and demonstrated (Zanger et al., 2011). It should be noted that gas turbines working in these coupled conditions are categorized as microturbines. These are derived from the auxiliary power units (25kW-500 kW) of large aircrafts and have high rotational speeds between 90,000 and 120,000 revolutions per minute (Soares, p 618).

---

## *Chapter Summary*

In this chapter, the gasification technology is introduced and various factors effecting the choice of gasifier are described. Additionally, the current state of the art for SOFC is highlighted. Further on, the hybrid operation of SOFC with gas turbine is briefly discussed.

#### *References:*

- Duret, Alexis, Claude Friedli, and François Maréchal. "Process design of Synthetic Natural Gas (SNG) production using wood gasification." *Journal of cleaner production* 13.15 (2005): 1434-1446.
- Higman, C., and M. Van Der Burgt. "Gasification." (2003).
- Himansu, Ananda, et al. "Hybrid solid oxide fuel cell/ gas turbine system design for high altitude long endurance aerospace missions." *Proceedings of FUELCELL2006, 4th International ASME Conference on Fuel Cell Science, Engineering and Technology*, June. 2006.
- Huijsmans, J. P. P., F. P. F. Van Berkel, and G. M. Christie. "Intermediate temperature SOFC—a promise for the 21st century." *Journal of Power Sources* 71.1 (1998): 107-110.
- Larminie, James, Andrew Dicks, and Maurice S. McDonald. *Fuel cell systems explained*. Vol. 2. New York: Wiley, 2003.
- Nikoo, Mehrdokht B., and Nader Mahinpey. "Simula-

tion of biomass gasification in fluidized bed reactor using ASPEN PLUS." *Biomass and Bioenergy* 32.12 (2008): 1245-1254.

Park, S. K., and T. S. Kim. "Comparison between pressurized design and ambient pressure design of hybrid solid oxide fuel cell-gas turbine systems." *Journal of Power Sources* 163.1 (2006): 490-499.

Singhal, S. C. "Advances in solid oxide fuel cell technology." *Solid state ionics* 135.1 (2000): 305-313.

Soares, Claire. *Gas Turbines: a handbook of air, land and sea applications*. Butterworth-Heinemann, 2011.

Tucker, Michael C. "Progress in metal-supported solid oxide fuel cells: A review." *Journal of Power Sources* 195.15 (2010): 4570-4582.

van der Meijden, Christiaan M., Hubert J. Veringa, and Luc PLM Rabou. "The production of synthetic natural gas (SNG): A comparison of three wood gasification systems for energy balance and overall efficiency." *Biomass and bioenergy* 34.3 (2010): 302-311.

Veyo, Stephen E., et al. "Tubular SOFC hybrid power system status." *ASME Turbo Expo 2003, collocated with the 2003 International Joint Power Generation Conference*. American Society of Mechanical Engineers, 2003.

Vitasari, Caecilia R., Martin Jurascik, and Krzysztof J. Ptasinski. "Exergy analysis of biomass-to-synthetic natural gas (SNG) process via indirect gasification of various biomass feedstock." *Energy* 36.6 (2011): 3825-3837.

Yang, Chenghao, et al. "Sulphur-Tolerant Redox-Reversible Anode Material for Direct Hydrocarbon Solid Oxide Fuel Cells." *Advanced Materials* 24.11 (2012): 1439-1443.

Zanger, Jan, Axel Widenhorn, and Manfred Aigner. "Experimental Investigations of Pressure Losses on the Performance of a Micro Gas Turbine System." *Journal of Engineering for Gas Turbines and Power* 133.8 (2011): 082302.

# Thermodynamics

Thermodynamics is most commonly described in forms of mathematical equations but has far more significant physical implications. The description of the law of conservation of energy for example, in mathematical form, is rather complicated as precision and the need to include all possibilities are highly desirable. The first law in its entirety can be described by the following equation (Sandler, 50):

$$\frac{d(U + m(v^2/2 + gz))}{dt} = \sum_k \dot{m}_k (\bar{H} + v^2/2 + gz) + \dot{Q} + \dot{W}$$

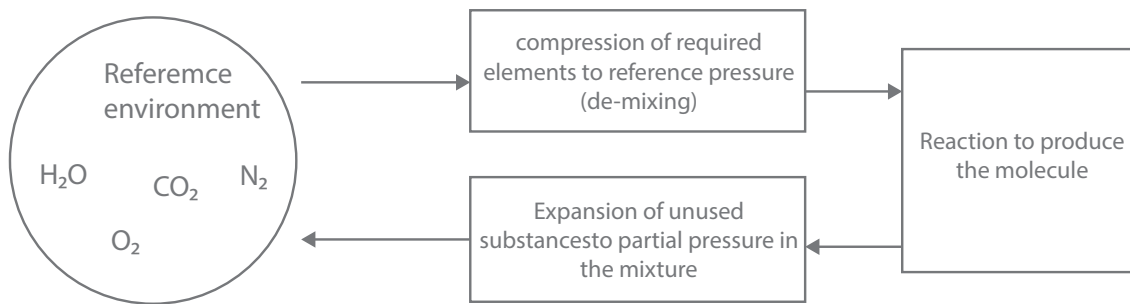


Figure 5 Steps for calculating the chemical exergy of a molecule. Adapted from (Martinez, 2011)

The term on the right describes the changes in the total energy of the system, which is the sum of internal, kinetic and the potential energy, with time. The first term on the right hand side of the equation describes changes in energy due to mass flows. In a closed system, mass flows do not contribute to energy change and thus this term equates to zero. Another commonly observed phenomenon is the preference of systems to attain a state of equilibrium. Given the condition that mass flows, heat and work transfer across the surface cease to exist and also given enough time, all processes must attain a state of equilibrium with their immediate environment. Mathematically, the equation above can be manipulated to describe the same message.

Taking it a step further, it is possible to measure the amount of reversible work that can be extracted when a system is brought from an initial state to a state of equilibrium with the immediate surroundings. A variable called exergy is defined which describes this work (Szargut et al.,) As this work is reversible, it is also possible to define exergy as the minimum amount of work needed to produce the energy carrier in its existing state from the substances in the inert reference state (Sato, 98). Unlike energy which is conserved in any process,

exergy is not. A spontaneous process occurring in the reference environment tends to decrease the exergy of the system.

The exergy of a substance is defined in two separate variables: physical exergy which is associated with changes in temperature, pressure and in concentration with respect to the reference environment; and chemical exergy is the exergy related to changes of chemical compositions.

## Exergy Calculations

The exergy for a substance can therefore be written as,

$$\varepsilon_{total} = \varepsilon_{ph} + \varepsilon_{ch}$$

Where  $\varepsilon_{ph}$  is physical exergy and  $\varepsilon_{ch}$  is the chemical exergy. As defined above, the chemical exergy is related to the exergy change associated with changing chemical composition. A simple procedure to calculate the chemical exergy from the reference environment is described in Figure 5

- To begin with, the components are demixed from their reference environment. The chemical exergy associated with de-mixing is  $\bar{R}T \ln x_i$ , where  $x_i$  is the molar fraction of the component  $i$  in the mixture. De-mixing is the compression of the components of standard air from their partial pressures to the atmospheric pressure under isothermal conditions.

- Next step in the calculation is the calculation of Gibbs free energy of formation of the molecule from the species present in the atmosphere. This is represented by  $\sum_i v_i \bar{g}_i$

- Finally the components must be expanded back to their partial pressures in the reference environment. Molar Gibbs free energy,  $g$ , can be calculated using the relation below:

$$\bar{g} = \bar{h} - T\bar{s}$$

The exergy efficiency of the system is describes as:

$$\eta_e = \frac{\sum \varepsilon_{out}}{\sum \varepsilon_{in}}$$

For the case of gasification plant, the equation above translates into:

$$\eta_e = \frac{\varepsilon_{SNG}}{\varepsilon_{biomass} + W_{in}}$$

In total, the gasification plant consumes power which is reflected in the equation above. Of particular significance is the denominator which shows addition of the exergy of biomass,  $\varepsilon_{biomass}$  and the work input,  $W_{in}$ . However, it is not defined how  $W_{in}$  is produced. It is possible to produce  $W_{in}$  from biomass in which case the  $W_{in}$  can be included with  $\varepsilon_{biomass}$ . A more realistic definition would consider the exergy contained in the source from which  $W_{in}$  is generated. However, for the current study exergy efficiency will be calculated as defined in the equation above.

For the SOFC-GT system the exergy efficiency can be calculated as follows:

$$\eta_e = \frac{W_{net}}{\varepsilon_{in, fuel}}$$

The exergy for a steady flow process for an open system is described as (Kaushik et.al., 2011):

$$P = \sum_k \left( 1 - \frac{T_0}{T_k} \right) \dot{Q}_k + \sum_k \dot{m}_k (\varepsilon_{in} - \varepsilon_{out})_k - T_0 \dot{S}_{gen}$$

$$\dot{W}_T = \dot{m}(\varepsilon_{in} - \varepsilon_{out}) - T_0 \dot{S}_{gen}$$

$$-\dot{W}_C = \dot{m}(\varepsilon_{in} - \varepsilon_{out}) - T_0 \dot{S}_{gen}$$

The first summation term on the right hand side of the equation represents the exergy available from heat flow. The second term on the right hand side of the equation describes the exergy available due mass flows and the final term on the right represents the exergy lost due to irreversibilities.

### Defining reference environments

Per definition of exergy, the reference state of the constituting substances determines the exergy of the final substance in any other state. In most thermodynamic calculations, the system operates at the sea level and therefore it is a natural choice of reference state. In the present study, the system operates at altitudes as high as 21 km. International standard atmosphere defines the temperature and pressures at the mentioned height. This data is helpful in determining the composition of the air. The variation of temperature, pressure till the tropopause at the height of 11000 m can be modelled

with the relation given below (Cavcar, 2000):

$$T = T_0 - 6.5 \left( \frac{h}{1000} \right)$$

$$p = p_0 \left( 1 - 0.0065 \left( \frac{h}{T_0} \right) \right)^{5.261}$$

After this height, the temperature is assumed to be constant at -56.5 °C. After that, the pressure variation is given by the relation below (Cavcar, 2000):

$$p = p_{11} e^{-\frac{g}{RT_{11}}(h-h_{11})}$$

Where the subscript '11' corresponds to the values at the limit of Tropopause. The Clausius - Clapeyron equation relation helps in calculating the saturation pressure for water vapours under temperature and pressure calculated using the equations above (Sandler, 319):

$$P_{sat}(T_2) = P_{sat}(T_1) \exp \left[ \left( -\frac{\Delta H}{R} \right) \left( \frac{1}{T_2} - \frac{1}{T_1} \right) \right]$$

The composition of the atmosphere can thus be calculated at different altitudes.

## Chapter summary

Basics for thermodynamic analysis are presented. The difference in operating conditions at higher altitude results in a different procedure for making thermodynamic analysis. This issue is discussed in detail in the current chapter.

### References

Cavcar, Mustafa. "The International Standard Atmosphere (ISA)." Anadolu University, Turkey (2000).

Kaushik, S. C., V. Siva Reddy, and S. K. Tyagi. "Energy and exergy analyses of thermal power plants: A review." Renewable and Sustainable energy reviews 15.4 (2011): 1857-1872.

Martínez I. "Chemical Exergy". UPM (2011). Web 26 Oct 2014. <<http://webserver.dmt.upm.es/~isidoro/>>

Sandler, Stanley I. Chemical, biochemical, and engineering thermodynamics. Vol. 4. Hoboken, NJ: John Wiley & Sons, 2006.

Sato, Norio. Chemical energy and exergy: an introduction to chemical thermodynamics for engineers. Elsevier, 2004.

Szargut, Jan, David R. Morris, and Frank R. Steward. Exergy Analysis of Thermal, Chemical, and Metallurgical Processes. New York: Hemisphere, 1988. Print.

# System Description

## Gasification System

In Chapter 1, the significance of biomass as an indispensable energy resource was presented. However, the utility of this resource is difficult to measure until it is converted into usable fuel. Based on the path for this conversion process, there are two ways of bringing about this change- thermochemical and biochemical pathways. Thermochemical pathways make use of chemical reactions taking place at elevated temperatures to bring about this change. Biochemical pathways rely heavily on enzymatic microorganisms to convert biomass into fuels in relatively moderate temperature and pressure environments. The reaction rates are much slower and thus it takes much longer to finish the conversion process. A detailed discussion on biochemical pathways is outside the scope of current study.

In the current study, compressed synthetic natural gas (SNG) is used in a SOFC-GT hybrid system. The first part of this study involves gasifying the biomass, cleaning it and producing syngas as one of the products. The scheme of the gasification and gas cleaning unit is shown in Figure 6. Before entering the methanation unit, the hydrogen to carbon monoxide ratio is adjusted in a high temperature shift reactor. Finally the syngas is converted into SNG. In the end, methane is separated from other components (carbon dioxide and water) and then compressed to 200 bar for storage. The flowsheet of the gasification plant is available in Appendix 4A.

In order to get the optimum results from the gasification system, a good starting point is the right biomass source. Birch wood was selected as the biomass source. The composition of birch wood can be noted in Table 2

Table 2 Birch wood composition (Phyllis, 2000)

Element	Weight %		
	As received	dry	Dry ash free
Carbon	43.29	48.70	48.88
Hydrogen	5.69	6.40	6.42
Nitrogen	0.07	0.08	0.08
Sulphur	0.00	0.00	0.00
Oxygen	39.52	44.45	44.62

Using existing literature, the amount of different gases produced during this gasification process is estimated. Simple atomic balances were carried out in spreadsheet software. The calculations are made available in Appendix 4B.

The compositions determined from this calculation are put into the gasifier model in Aspen. The gasifier is modelled as two separate units of gasification and combustion reactors. Appendix 4A shows the flowsheet of the gasifier and gas cleaning unit. The working temperature and pressure for different blocks can be noted in Table 3. After the gasification is complete, the product gases are taken in a char separator where ashes and char are separated and fed to the combustor. The remaining gases are sent to the gas cleaning section. The gas cleaning section is composed of a high temperature filter, sulphur filter and a scrubber. High temperature filters make use of candle filters that remove all of the

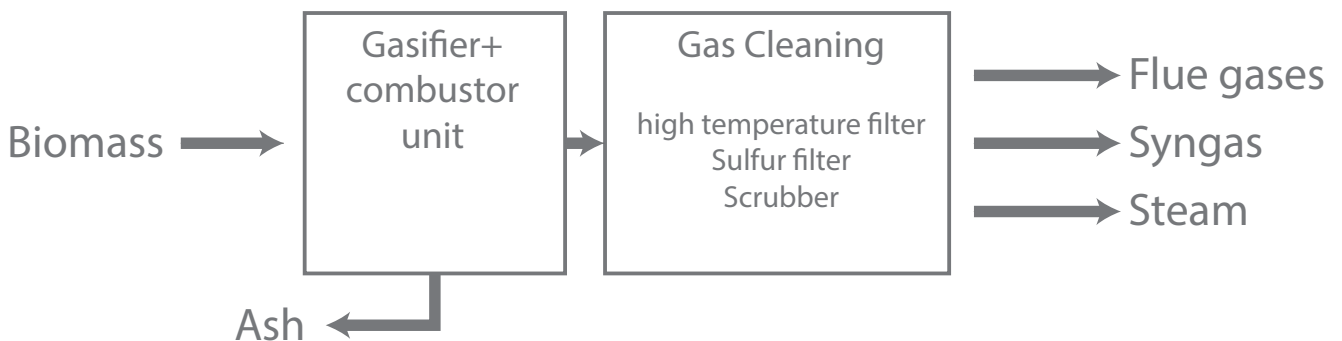


Figure 6 Scheme for production of Syngas

solid particulates from the syngas (Heidenreich, 2013). They are usually made up of ceramic material that can retain mechanical strength at high operating temperatures (Higman et al., 2003). The desulfurization unit is a fixed bed reactor filled up with zinc oxide. In the high temperature product gas from the gasifier, sulphur is present mostly in the form of H<sub>2</sub>S and adsorption of H<sub>2</sub>S into ZnO results in syngas with <0.1 ppmv purity. The bed has to be replaced from time to time as in situ regeneration is not possible (Higman, 2003). A wet scrubber is used for removing particles of less 10 microns in size with the help of a liquid that condenses on the particle surface. The syngas is fed through a throat section which accelerates the flow and the particles are separated further downstream because of turbulence (Rezaiyan et al., 2005).

Table 3 Component specifications for different reactor blocks in ASPEN

Component	Value	units
Gasifier (Yield Reactor)		
Temperature	850	C
Pressure	1.3	bar
Combustor		
Temperature	920	C
Pressure	1.3	bar
HT Filter	Temperature	850 C
S Filter	Temperature	400 C
Scrubber	Temperature	47 C
	Pressure	1.18 bar

The heat from the combustor is carried to the gasification reactor. However, this separation of combustion and gasification reactors is done only for simulation. The steam required for gasification is made available by using the heat in the flue gas. Table 4 shows internally generated steam for the gasification plant.

Table 4 Process steam generated in the gasification system for different reactors.

	Temperature( °C)	Pressure (bar)
Gasifier	400	1.3
High temperature Shift reactor	350	1.6

### Methanation system description

As mentioned in earlier chapters, methanation process has been studied in various configurations. For this study, adiabatic fixed bed methanation has been carried out for synthesis of methane from syngas based on the ICI process (Imperial chemical industries) . The scheme for the simulation is shown in Figure 7. The methanation reactors are denoted by MR. The input flows to these process are steam and syngas in as shown in the scheme in the figure (Heyne et al, 2010). The outlet from the first methanation reactor is split to recirculate back in the methanation reactor to control the input temperature of the reactor. The remaining two reactors are provided with intercooling to limit the inlet temperatures of the feed gas going into the reactors. The intercoolers are set to limit the inlet temperature of the feed streams to 450 °C, 300 °C for the reactors 2 and 3 respectively. The flowsheet for the methanation plant is available in Appendix 4C. The methanation reactors are modelled in restricted equilibrium with temperature approach.

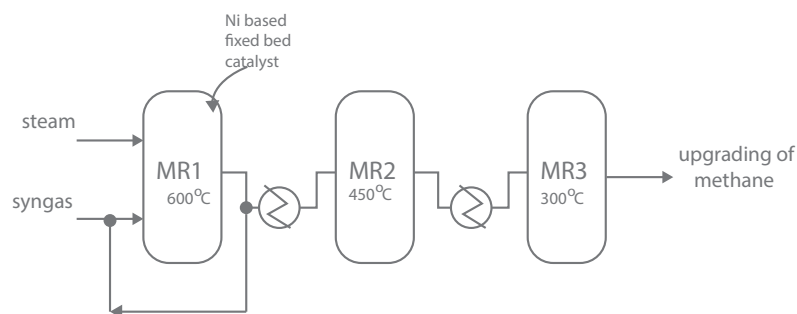


Figure 7 Adiabatic fixed bed methanation reactor scheme. (Heyne et. al, 2006)

The steam required for methanation reactor is produced internally at 300 °C and 18 bar. The product gas yield of methanation reaction has large amounts of steam and carbon dioxide. These components in the gas mixture are removed further down the stream.

Water is removed by cooling the gas mixture to a temperature of 80 °C in a condenser. In the next step, CO<sub>2</sub> is removed before sending it to the compressors using Selexol process. Selexol process is a chemical absorption based process where in CO<sub>2</sub> is selectively removed in a solvent. The solvent can be regenerated afterwards. The absorption depends on the partial pressure of the component (Higman et al., 2003). Therefore a lot of compression work is required. The compressors compress the methane to 200 bar at 25 °C. This is done in two stages with intercooling.

### SOFC-GT Hybrid system description

The unmanned aerial vehicles (UAV) propulsion system will be powered by a solid oxide fuel cell (SOFC) -gas turbine (GT) hybrid system. The fuel for this system will be generated in the gasification plant as described previously. It is now possible to simulate the functioning of the power delivery of the UAV. This section describes the models that were set up for the simulation in Cycle-tempo. The power delivery simulations are carried out in two parts- firstly the taking off of the aircraft and then the cruising stage. The objective in these simulations is to size the system based on the power required for taking off conditions. Subsequently the performance of the system is studied during cruise conditions. A large proportion of the required power is produced in the SOFC. The SOFC is modelled as a direct internally

reforming (DIR) SOFC. In this hybrid system, gas turbine functions as the bottoming cycle. The exhaust from the fuel cell is fed to the gas turbine to produce additional power. Figure 8 shows the scheme of the hybrid system operation.

Based on the altitude of operation, the definition of atmospheric air has to be changed. This also affects the amount of preheating and/or compression work required to provide the ingredients of right quality to the fuel cell.

Power required during take-off is more than that during cruise. This indicates that the system should be sized for taking off conditions. System for taking-off is modelled with the following input conditions as shown in Table 5

Table 5 Input parameters for SOFC-GT design condition simulation

Parameter	Value
SNG Storage Temperature (°C)	25
Compressor isentropic efficiency	0.75
Compressor mechanical efficiency	0.98
Generator efficiency	0.95
Gas turbine isentropic efficiency	0.8
Gas turbine mechanical efficiency	0.98
Environment temperature (°C)	25
Environment pressure (bar)	1.01325
ΔT Cathode (°C)	84.04

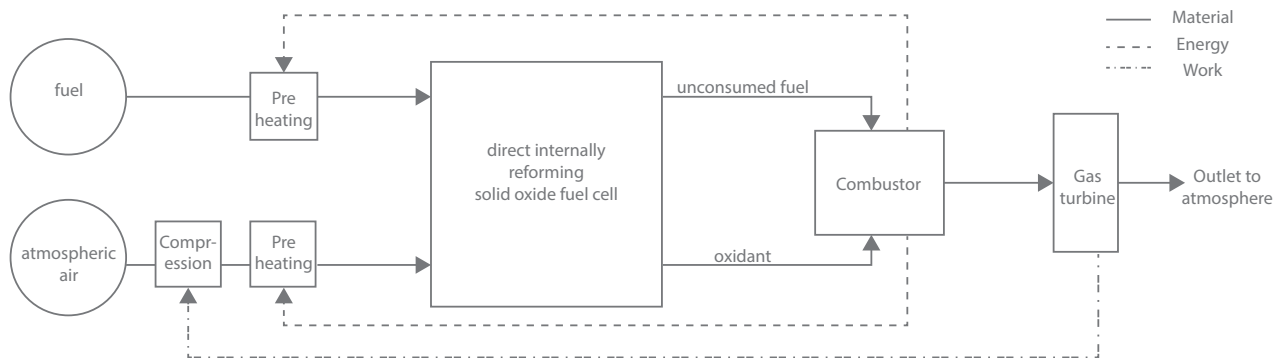


Figure 8 Scheme of SOFC-GT hybrid operation



<i>Parameter</i>	<i>Value</i>
$\Delta T$ Anode (°C)	100
SOFC Temperature (°C)	800
SOFC Pressure (bar)	1.5 to 5
maximum current density (A/m <sup>2</sup> )	5000
Are specific resistance ( $\Omega \cdot \text{cm}^2$ )	.29
Fuel Utilization	68%
SOFC Output (kW)	116.9

Among the parameters mentioned in Table 5, SOFC pressure is varied to determine understand the variation of efficiency and size of the system. In cycle tempo, this is done by specifying the anode and cathode inlet pressure. Along with these two variables, the pressure of the fuel cell and the reforming reaction pressure have to be modified. These simulations are performed for design conditions of take-off. The flow sheet is available in Appendix 4D. The flow sheet shows two configurations of air preheaters -A and B. Off-design operation during cruise is studied differently. The operating current density and cell voltage are varied to get the same cell area and area specific resistance as determined during design calculations. The atmospheric conditions at the cruise altitude demand the use of multi stage compressors and turbine. The intermediate pressure in the compressors is 0.263 bar and that in the turbine is 0.35 bar

## System Sizing

This study can be categorized as a design or sizing problem (Himansu et al., 2006). The flow properties at the inlet are already defined based on the environment conditions existing during operation. Also, the properties at the outlet are known because a defined amount of work has to be extracted from the system. The task, therefore, in this design problem is to determine the geometric size of the components that will generate the prescribed amount of work. A thermodynamic analysis will be used for estimating irreversibilities in the system. This analysis provides a good starting point in selecting the right kind and size of a component. The main system components are SOFC Stack, gas turbines, compressors, Electric motor, heat exchangers, fuel tank and combustor. Additional components include the piping, the valves and splits and joints.

Sizing analysis conducted by Himansu et al. also showed the critical parameters affecting the mass of the system. The mass of the system is a combination of all the components mentioned above and also the fuel mass. It was reported that for long duration missions (20 days), the most dominant components are the fuel (liquid hydrogen- LH<sub>2</sub>), LH<sub>2</sub> tank and SOFC stack, in that order. It can thus be concluded that high operating efficiency is the most important factor in reducing the system and size and increasing the operation time. An important consequence of this fact is that the operating power density will be lowered.

The system design is based on the concept proposed by NASA (Nickol et al., 2007). A heavier than air aircraft was proposed that would run on a proton exchange membrane fuel cell using liquid hydrogen as fuel. The mass constraints as set in the study are made available in Appendix 4E. For the purpose of current study, only the mass available for the propulsion system is considered. The mass of the aircraft structural elements are assumed to be similar. For sizing the system, the total mass is taken into account instead of the individual mass of the SOFC stack, turbocharger etc. The mission requirements are also taken from literature (Aguilar et al., 2008). These requirements are listed in the Table 6

Table 6 Mission requirements for the HALE UAV

<i>Paramter</i>	<i>Value</i>
<i>Cruising Altitude</i>	21 km
<i>Total take-off mass</i>	4922 kg
<i>Lift to drag ratio cruise</i>	40
<i>Take off power required</i>	240 kW
<i>Cruise power required</i>	100 kW

In order to calculate the endurance of the aircraft, the average energy content of the fuel is estimated using the fuel flow rate in the SOFC-GT plant. The average mission power requirements are assumed to be equal to that at cruise. A more realistic approach can include the actual mission profile which would differ from application to application. The endurance is given by:

$$endurance = \frac{Fuelmass}{\dot{m}}$$

---

## Chapter Summary

In this chapter, a description of the computer models for the gasifier, methanation and SOFC-GT units is laid out. ASPEN is used for modelling the gasification and methanation processes, whereas Cycle-Tempo is used for modelling SOFC-GT system. SOFC-GT system model parameters are mentioned for off-design and design conditions. Also two air preheater configurations are specified. Finally the constraints for the sizing the system are specified and the equation for calculating endurance is also specified.

### References

Aguiar, P., D. J. L. Brett, and N. P. Brandon. "Solid oxide fuel cell/gas turbine hybrid system analysis for high-altitude long-endurance unmanned aerial vehicles." *International Journal of Hydrogen Energy* 33.23 (2008): 7214-7223.

Heidenreich, Steffen. "Hot gas filtration—A review." *Fuel* 104 (2013): 83-94.

Heyne, Stefan, Martin Seemann, and Simon Harvey. "Integration study for alternative methanation technologies for the production of synthetic natural gas from gasified biomass." *Chemical Engineering Transactions*. 13th International Conference on Process Integration, PRES 2010. Vol. 21. 2010

Higman, C., and M. Van Der Burgt. "Gasification." (2003).

Himansu, Ananda, et al. "Hybrid solid oxide fuel cell/gas turbine system design for high altitude long endurance aerospace missions." *Proceedings of FUELCELL2006, 4th International ASME Conference on Fuel Cell Science, Engineering and Technology*, June. 2006.

Nickol, Craig L., et al. "High altitude long endurance UAV analysis of alternatives and technology requirements development." (2007).

"Phyllis2." - ECN Phyllis Classification. Web. 28 Aug. 2014. <[https://www.ecn.nl/phyllis2/Browse/Standard/ECN-Phyllis#birch wood](https://www.ecn.nl/phyllis2/Browse/Standard/ECN-Phyllis#birch%20wood)>.

Rezaiyan, John, and Nicholas P. Cheremisinoff. *Gasification technologies: a primer for engineers and scientists*. CRC press, 2005.

# Results and discussions

## Gasification Plant - Well to Tank Analysis

Determining the exergy flows in various processing sub-steps helps in developing understanding for the functioning of the system. The first system that was studied was the gasification and methanation unit as described previously (see Chapter 3). Table 7 below summarises the irreversibilities in different stages of processing. Figure 9 gives a clearer picture on the relative losses in these stages.

Table 7 Irreversibilities in gasification plant for the production of compressed SNG

Plant unit	Exergy Loss (KW)	Derived Work(kW)
Gasification	9472.09	
Gas Cleaning	2759.59	1200.00
High temperature Shift Reaction	189.12	
Methanation Reactor 1	2674.79	-3317.00
Methanation Reactor 2	1720.71	
Methanation Reactor 3	707.66	
Condensation	1691.09	
CO <sub>2</sub> separation	4384.89	-4512.80
Compressor Storage	216.06	-462.00
Stack	790.63	

Clearly, major irreversibilities are encountered during gasification process as it involves various combustion reactions mentioned before (see chapter 2). It has to be mentioned that not all products of the gasification reaction are useful and therefore significantly reduce the available exergy at the outlet. Unconverted carbon and formation of ashes imply that their exergies will be excluded from

the total useful exergy available at the outlet. Similar observations can be made in the products for the gas cleaning section. Together, these two stages account for 49% of the total irreversibilities in the compressed SNG production plant. It should be noted that sufficient measures have been taken to ensure that all the steam required for the processing is generated internally. Aided by the high temperature heat available in the flue gases and feed stream for gas cleaning, steam was generated for the gasification reactor and high temperature shift reactor. In addition, superheated steam at 20 bar and 650 °C was generated to drive a steam turbine, thereby producing 1.2 MW of power.

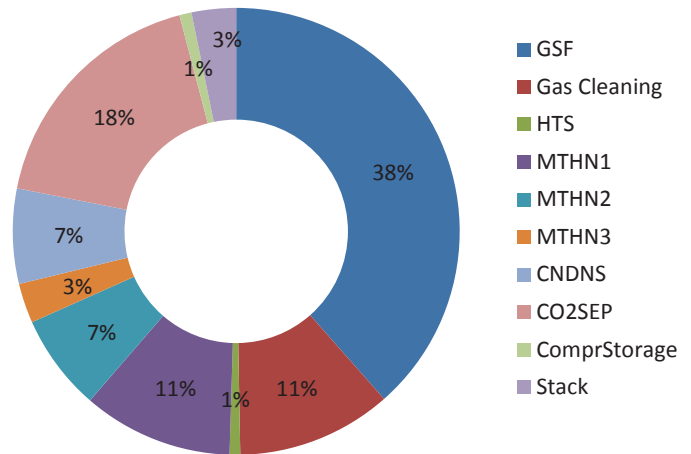


Figure 9 Breakdown of irreversibilities during production of compressed SNG in the gasification plant.

Adequate provisions were made to limit the temperature of the flue gas sent to the stack to close to 150 °C which is to avoid condensation of sulfur compounds. The other major contributing step to irreversibility is the carbon dioxide separation unit. The power consumed of the carbon dioxide removal process is estimated to be more than 4 MW (Vitasari et al., 2011).

After the shift reaction, the product gas is pressurized to 18 bar. This results in significant exergy losses as indicated in Table 7. Also most of the CO (more than 90%) conversion takes place in methanation reactor 1. For the subsequent methanation reactors, the reactor temperature are kept lower than for the first reactor. Correspondingly, the exergy losses decrease in the subsequent reactors after the first one.

Following the methanation reactors, the product gas is refined to increase the amount of methane content. First of all, the water is condensed out at 80 °C, which

results in large exergy losses. The product gas mixture at 80 °C is now fed to a CO<sub>2</sub> separation unit. As explained before selexol process consumes a lot of power and is therefore responsible for 18% of the total exergy losses. At this stage the product gas consists of just under 96% methane.

The final step is the compression of the SNG to 200 bar for storage. The flow quantity at this stage is reduced to almost 16 % of the feed at the start of methanation. (see appendix 5A). The exergy losses in this step is relatively lower than those in the first methanation reactor.

Figure 10 indicates the exergy flows in the production of compressed SNG. Also indicated are the fraction of exergy losses in the process. External work and biomass are the put into the process and the useful product is the compressed SNG which is 59.7% of the total input exergy, which is also the exergy efficiency of the compressed SNG production process from biomass.

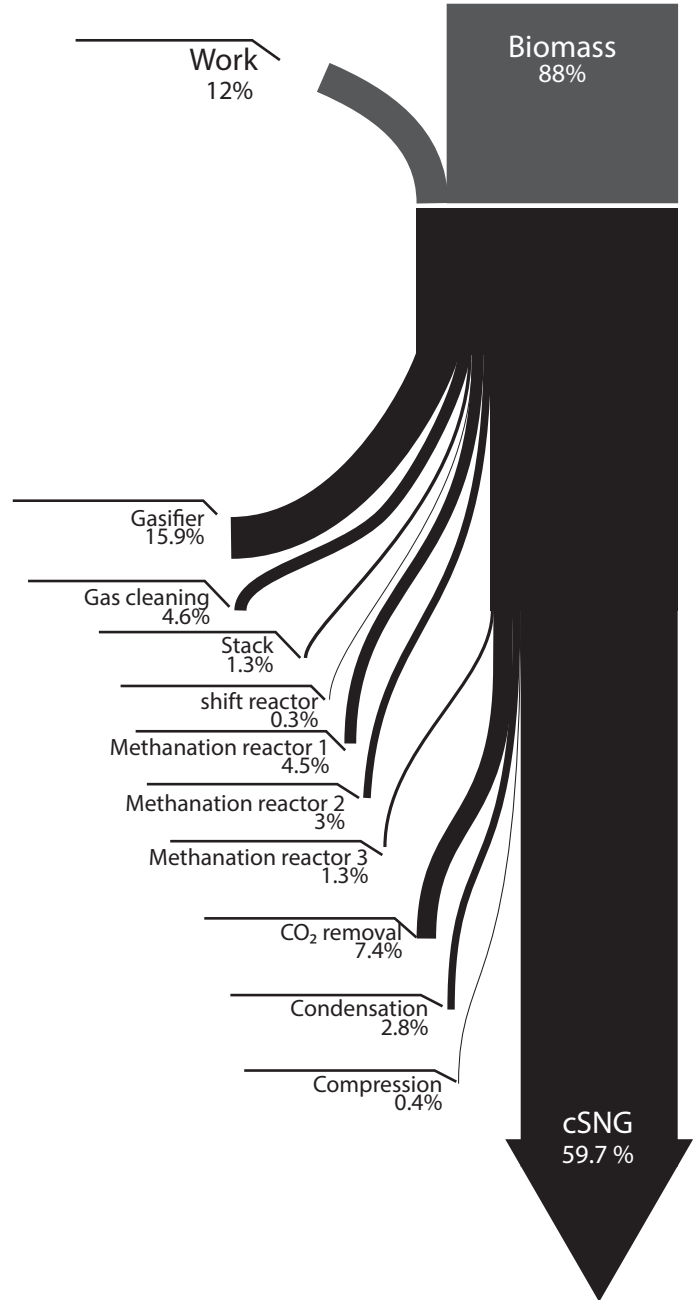


Figure 10 Grassman diagram depicting exergy flows in compressed SNG production

### SOFC -GT system - Tank to Wheel analysis

*Design conditions- take off*

The propulsion system for the aircraft has an estimated power requirement of 240 kW during takeoff and 100 kW during cruising conditions. The solid oxide fuel cell- gas turbine hybrid system is designed for takeoff conditions. Under these conditions and the selected fuel cell power density and current, a sensitivity study is carried to determine the system size for different fuel cell operating pressures. The operating pressure for the fuel cell is varied from 1.5 to 5 bar as shown in the Table 8.

As the operating pressure for the fuel cell increases, the Nernst potential of the cell increases and thus the efficiency increases. This variation is evident from the Nernst equation. Also in the same fashion the area of the fuel cells required to meet the design conditions drops. The area of the cell required under various operating pressures are also shown in the Table 8. A plot showing the gain in efficiency of SOFC-GT hybrid system is shown in Figure 11. It is evident that the incremental gains in efficiency start saturating at pressure of 5 bar. It can be concluded that an operating pressure of 5 bar reduces the system size by more than 9% (see Table 8).

Table 8 Sensitivity analysis of SOFC-GT system with different operating pressures

Fuel cell operating pressure (bar)	Exergy Efficiency (%)	Area of the fuel cell (m <sup>2</sup> )
1.5	55.8	31.0
2	57.4	30.1

Fuel cell operating pressure (bar)	Exergy Efficiency (%)	Area of the fuel cell (m <sup>2</sup> )
2.5	58.6	29.6
3	59.5	29.1
3.5	61.4	28.7
4	62.0	28.4
4.5	62.5	28.2
5	62.9	28.0

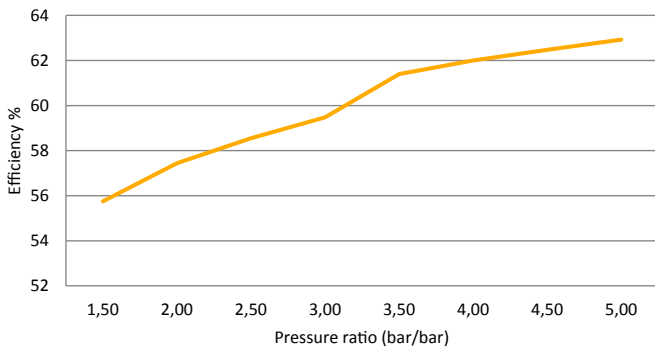


Figure 11 Plot showing the results of sensitivity analysis. Efficiency is plotted against the SOFC operating pressure.

*Off-Design conditions - Cruise*

At this point, it will be good to remember that any reduction in system size implies an increased capacity for fuel storage, so that the endurance of the aircraft increases. Under off-design conditions of cruising, the system is supposed to perform at an altitude of 21 km. The atmospheric composition in such conditions is available in appendix 5.B The power required in such conditions is reduced to 100 kW. The exergy calculations in non-standard environments are made as per the discussion in chapter 3. Furthermore, the position of the air preheater can be changed to alter the turbine inlet temperature. Two different configurations have been discussed in chapter 4. The results from exergy calculations are summarized in Table 9:

Table 9 Exergetic Efficiency(%) and Area(m<sup>2</sup>) of SOFC-GT system operation in different conditions. A and B refer to two configurations of air preheater.

Pressure	Take-off		Cruise		Area(m <sup>2</sup> )	
	A	B	A	B	A	B
1.5	57%	57.3%	68.9%	70.1%	31.0	30.3
5	64.2%	64.5%	68.2%	69.6%	28.0	27.5

It is clear that increasing the operating pressure of the fuel cell in design condition increases the exergetic efficiency of the hybrid system. For both the configuration A and B of the air preheater, the larger system has a higher efficiency. This can be seen in Table 10. Comparing system 1.5-B and 5-B, the difference in efficiency is a slightly more than 0.5 %. However, there is a reduction in system size by 9.6%. It can also be seen that the oxidant utilization is lower in system 5-B which is compensated by having a larger air flow rate. Consequently, the compression work is higher and the power at the generator is lesser for system 5-B. In order to produce the same total power (50 kW), system 5-B produces more power in the fuel cell. This therefore demands a higher fuel flow rate. Comparing systems 1.5 - A and 5- A, similar conclusions can be drawn.

While comparing the two configurations of the air preheater, it can be seen that the power available at the generator is higher for configuration B than for configuration A( by around 8%). The turbine inlet temperatures for GT1 is also higher for configuration B and the corresponding the exhaust gas temperature at the stack is lower for configuration B than for A for both the system sizes. This effect can also be seen at the power available at the generator. Configuration B has much higher power available at the generator.

Table 10 A comparison of Performance parameters for SOFC-GT hybrid system during off-design conditions.

	1.5-A	5-A	1.5-B	5-B
Fuel cell voltage (V)	0.87	0.87	0.87	0.87
Fuel Utilization	0.71	0.71	0.71	0.71
Oxidant utilization	0.46	0.44	0.45	0.41

	1.5-A	5-A	1.5-B	5-B
Area specific resistance ( $\Omega.cm^2$ )	0.28	0.29	0.29	0.29
current density ( $A/m^2$ )	1705	1895	1725	1898
Fuel cell pressure (bar)	1.47	1.47	1.47	1.47
Fuel flow rate (g/s)	1.40	1.41	1.38	1.39
air flow rate (g/s)	26.09	27.00	25.96	28.39
Net turbine power (kW)	6.83	6.80	7.44	7.29
Fuel Cell Power (kW)	43.80	43.80	43.10	43.26
Auxiliary power consumption (kW)	0.59	0.60	.589	.543
Power at generator (kW)	50.04	49.99	50	50
exergetic efficiency (%)	68.90	68.20	70.15	69.61

	1.5-A	5-A	1.5-B	5-B
GT1 TIT ( $^{\circ}C$ )	1043	1032.17	1188.51	1161.97
GT1 TET ( $^{\circ}C$ )	709.28	700.00	834.07	810.87
GT2 TIT ( $^{\circ}C$ )	709.28	700.00	676.30	637.35
GT2 TET ( $^{\circ}C$ )	444.82	437.84	419.00	388.46

It should be clearly noted, however, that during off design conditions the SOFC system is operated at a pressure of 1.47 bar. The pressures indicated in the table above are only used for design conditions. Also, the power delivered at the generator is the net power available from the turbines after accounting for the power used by compressors which are mounted on the same shaft.

The operation of the hybrid system during off design conditions provides various avenues for critical remarks. The atmospheric composition at higher altitude is one among many parameters affecting the functioning of the system. A summary of the exergy analysis and naming convention used in the figure is available in Appendix 5.C. The calculated irreversibilities for the hybrid system are plotted in the Figure 12.

Major irreversibility is encountered in the stack. It should be noted that this is the exergy that is lost to the external environment rather than destroyed. Apart from that, there are major losses in the generator due to electro-mechanical irreversibilities in electric auxiliaries, compressors and turbines. Losses in the combustor and fuel cell are other significant contributors to exergy destruction. The effect of the position of the

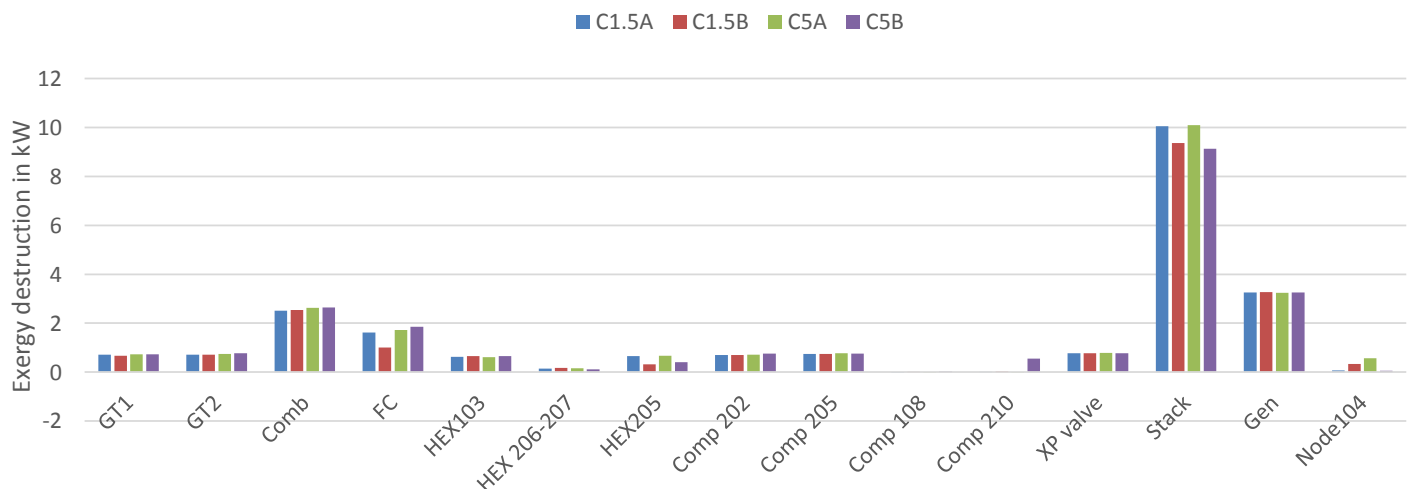


Figure 12 Irreversibilities in different components during off design operation of the hybrid system. In the legend, C stands for cruise, (1.5/5) shows the operating pressure during take off and the configuration of air preheater (A/B).

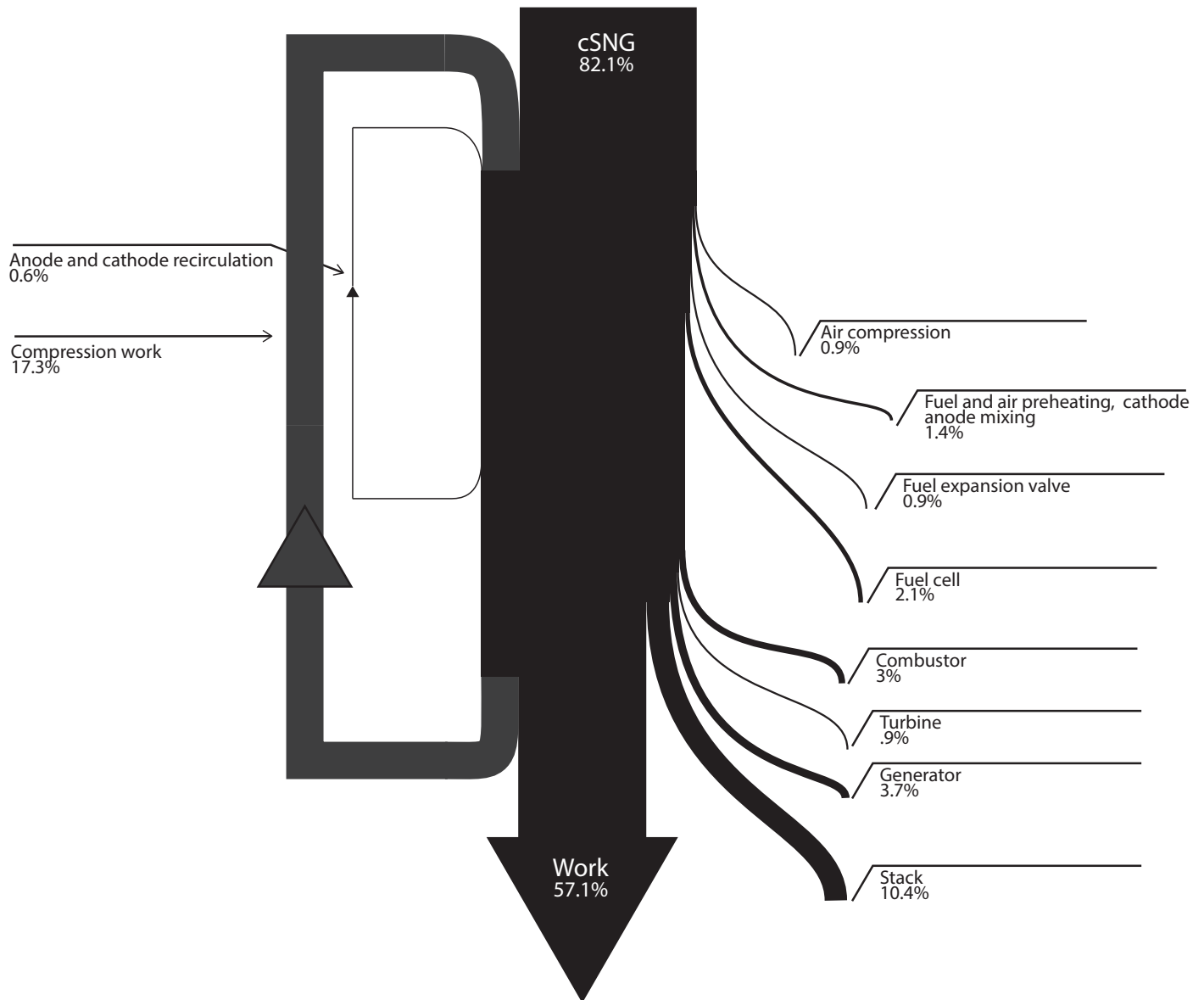


Figure 13 Grassman diagram for the SOFC-GT system operating in off-design conditions (in cruise reference environment) with air preheater configuration B.

air preheater (HEX 205) can also be seen in the Figure 12. For configuration A, the exergy losses are higher than those for configuration B. This is true for both system sizes, with design pressure of 1.5 and 5 bar. Figure 13 shows the Grassman diagram for the SOFC-GT system. A part of the work from the gas turbines is recirculated to power the compressors for the inlet air and also the cathode and anode recirculation flows. The system produces enough work to power the compressors for inlet air and recirculation circuits for anode and cathode.

## System Sizing

### Mass estimation

Based on the constraints defined in chapter 4, different components for the propulsion system for the aircraft were identified. The Turbochargers were sized for a power requirement of 15 kW peak. Since this power range is not readily available, based on the system sizes available, power was plotted against specific power as shown in Figure 14. Upon extrapolation, it can be seen that a specific power of .45 kW/kg would be available for a 15 kW turbocharger system.

Fuel cells were sized based on the generation 3 stack from Delphi with a power density of .278 kW/kg. The stack uses anode supported cells that have an area specific resistance of .29 Ωcm<sup>2</sup> (SOFC Power, ASC 800). Heat exchanger mass is calculated based on the available weight estimates (Santarelli, 2008). Heat exchanger area is calculated using ε-NTU method and also based on the commercial units available (Triboix, 2009), (Heatric, 2014). The CNG tanks are also sized based on commercial units (Quantum technologies, 2014). Synchronous 3 phase electric motor available from McLaren technologies is used (McLaren, 2014). Table 11 summarizes the mass distribution for different components in the system.

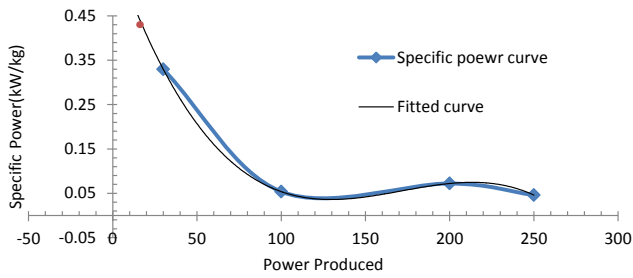


Figure 14 Specific power of turbochargers plotted against the net power produced (Capstone), (Turbec), (Elliot).

Table 11 Mass of different components in th propulsion system

Component	Mass (kg)
SOFC	1005.7
Turbocharger	139.5
Electric Motor	77.0

Component	Mass (kg)
Inverter	240.0
Heat Exchangers	63.9
Available fuel +tank mass	1312.9
Total Mass ( including fuel)	2839
Fuel mass in the system	553.4

With the proposed SOFC –GT hybrid system, a total of 46% of mass is available fuel and tank out of the total mass available for the plant. However, CNG cylinders for storing SNG have a total mass greater than the total SNG itself. It is also possible to estimate the mission endurance. Depending on the altitude of operation and cruising speed, the thrust specific fuel consumption of the aircraft can be calculated. An estimate is made for the flight endurance using equation described in Chapter 4.

The SOFC-GT system power train that will power the propellers is explained in the scheme in Figure 15. Two turbochargers are used for supplying the air at the necessary pressure to the SOFC unit ( Delphi, 2008). The SOFC produces DC power which has to be converted to AC power in an inverter. The power from the gas turbines is also combined to the power from the inverter and is used to drive the motor unit (McLaren, 2014).

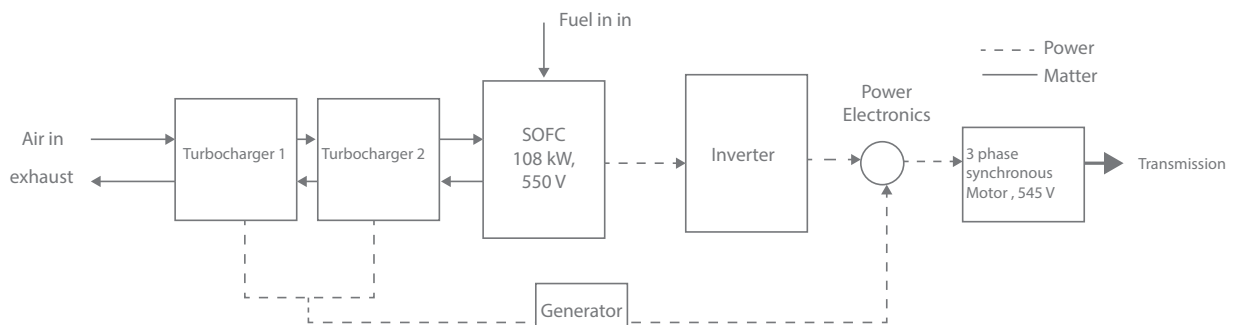


Figure 15 Power train for the SOFC-GT system for powering the UAV.



*Volumetric Sizing*

It should be noted that the the power electronics system that will drive the propeller is not modelled in this study. The component dimensions are based on the literature as sited in the mass sizing. These are summarized in Table 12.

Table 12 Component sizes for the nacelle assembly. W = width, L= length, D= diameter, H=height.

<b>Component</b>	<b>Dimensions (in m)</b>
Turbocharger( WLH)	.76 x 1.5 x 1.8
Electric motor (D, L)	.185, .254
CNG Tank (D,L)	.648, 2
Air preheater (WLH)	.8 x .4 x .04
Fuel preheater (WLH)	.2 x .5 x.02
Inverter (WLH)	.2 x .5 x.9
SOFC (WLH)	.103 x .103 x .24

Figure 16 shows the assembly of the components mentioned above in the nacelle of the UAV.

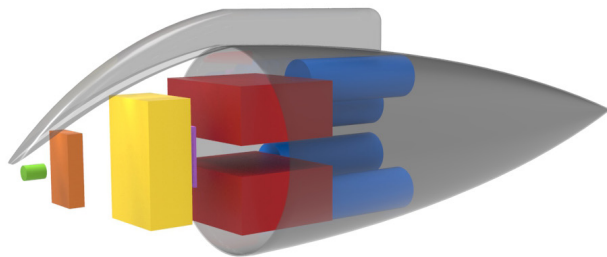


Figure 16 Assembly of components in the nacelle. Electric motor is shown in green, inverter in orange, SOFCstack in yellow, turbochargers in red and CNG tanks in blue. Heat exchanger is in purple.

*Comparison with liquid H<sub>2</sub> systems*

Previous research on liquid hydrogen systems for the same propulsion concept has been undertaken (Fernandes et al., 2014). A 'well-to-wheel' comparison can be made for these two systems based on the parameters defined in the Table 13:

Table 13 Comparison of performance paramters for the liquid hydrogen and compressed SNG systems for powering the HALE UAV.

	<b>LH<sub>2</sub></b>	<b>compressed SNG</b>	<b>unit</b>
<i>Fuel production efficiency</i>	18.8	59.7	%
<i>SOFC-GT system efficiency</i>	57.6	69.6	%
<i>Fuel Consumption</i>	1.29	2.77	g/s
<i>'Well-to-wheel' efficiency</i>	11.3	41.6	%
<i>Endurance estimate</i>	4.96	2.31	days

The fuel production efficiency for liquid H<sub>2</sub> plant is significantly lower than compressed SNG plant mainly because of high amount of work input for liquefaction unit. The efficiency of the liquefaction plant was estimated to be 40%. In the current system, SNG is compressed to a pressure of 200 bar which requires lesser amount of energy input. The efficiency of the system during off-design conditions of cruising is also lower for the liquid H<sub>2</sub> system.

An important remark for the thermodynamic analysis undertaken for the liquid hydrogen systems is that electrolyte- supported cells were used to meet the power demands. The operating current density for such cells is limited to 2500 A/m<sup>2</sup> during take-off. Moreover, sizing studies were not undertaken and it is estimated that the hydrogen design may not meet the weight requirements of the aircraft. However, it can be noted that future studies which will use of anode- supported cells will operate at higher current densities – closer to 5000 A/m<sup>2</sup> which would mean that the efficiency will drop further. It does imply that the comparison of these two fuel options is not even on all grounds but in terms of delivered performance, compressed SNG as fuel provides a higher 'well- to-wheel' efficiency. The endurance is estimated based on the assumptions described in chapter 4. In order to calculate the endurance for the LH<sub>2</sub> system, it was assumed that the aircraft can carry the same amount of fuel as that by the aircraft working on compressed SNG. The fuel consumption rate for LH<sub>2</sub> is 46.6% that of compressed SNG system and correspondingly the endurance is higher by the same amount. But in real terms, the LH<sub>2</sub> powered aircraft can carry much more fuel which would increase its endurance.

## Chapter Summary

The results from exergy calculations are described in this chapter. In the gasification plant, the major exergy losses are in the gasifier, CO<sub>2</sub> separation, gas cleaning and the methanation unit. Together they account for 78% of the exergy losses. The exergetic efficiency for compressed SNG production is 59.7%. The SOFC-GT system is studied for design conditions and a sensitivity analysis is carried out to determine the optimum system size. Further on, the system performance is analysed during off-design conditions of cruise with two different sizes and two configurations of air-preheaters (noted by 1.5 /5- A /B). The smaller system with configuration B is chosen as the best in the lot with an exergetic efficiency of 69.6%. Finally, system sizing is carried out to verify if the system indeed fits in the nacelle volume as given in the aircraft design specifications. As was expected, the system does fit in the volume and the endurance of the system was estimated to be 2.3 days.

### References

- Delphi Gen 3 stack. Web 18 Oct 14.  
< <http://www.netl.doe.gov/file%20library/events/2008/seca/presentations/Shaffer.pdf> >
- Capstone C30. Web 28 Sept. 14. <[http://www.capstoneturbine.com/\\_docs/datasheets/C30%20NatGas\\_331031E\\_lowres.pdf](http://www.capstoneturbine.com/_docs/datasheets/C30%20NatGas_331031E_lowres.pdf) >
- Elliot TA-100. Web 28 Sept. 14.  
< <http://www.helioselectric.com/manuals/microturbines/ta-100.pdf> >
- Fernandes, A et al. "Thermodynamic analysis of use of biomass-derived liquid hydrogen for a solid oxide fuel cell-gas turbine-powered aircraft." 2014. TU Delft.
- Heatric. Web 15 Oct. 2014.  
<[http://www.heatric.com/typical\\_characteristics.html](http://www.heatric.com/typical_characteristics.html)>
- "E-Motor." McLaren Applied Technologies. Web. 21 Oct. 2014. <<http://www.mclarenelectronics.com/Products/Product/E-Motor>>.
- Quantum technologies. Web 18 Oct 14.  
< [www.qtww.com/assets/u/CNGTankSpecificationsFeb2013.pdf](http://www.qtww.com/assets/u/CNGTankSpecificationsFeb2013.pdf) >
- Santarelli, Massimo, M. Cabrera, and Michele Cali'Quaglia. "SOFC-based systems as APU for different aircraft typologies: feasibility analysis and problems." (2008).
- SOFC Power. Pergine Valsugana: SOFC Power, n.d.

SOFC Power. Web. 22 Sept. 14. <[www.sofcpower.com/uploads/File/products/asc-700\\_asc-800.pdf](http://www.sofcpower.com/uploads/File/products/asc-700_asc-800.pdf)>.

Triboix, Alain. "Exact and approximate formulas for cross flow heat exchangers with unmixed fluids." *International Communications in Heat and Mass Transfer* 36.2 (2009): 121-124.

Turbec T100. Web. 28 Sept. 14.  
< [http://www.ensola.com/cms/images/stories/2012\\_inhalte/pdf/technical\\_description\\_t100\\_e\\_.pdf](http://www.ensola.com/cms/images/stories/2012_inhalte/pdf/technical_description_t100_e_.pdf) >

Vitasari, Caecilia R., Martin Jurascik, and Krzysztof J. Ptasiński. "Exergy analysis of biomass-to-synthetic natural gas (SNG) process via indirect gasification of various biomass feedstock." *Energy* 36.6 (2011): 3825-3837.

aircraft powered by LH<sub>2</sub>

# Conclusions

## Summary

A thermodynamic analysis was presented for a solid oxide fuel cell – gas turbine hybrid system. A well to wheels study was made for using compressed synthetic natural gas for powering an unmanned aerial vehicle. Starting from biomass, syngas was produced in a fast internal circulated fluidised gasifier. This gasifier produces syngas that is cleaned by removing sulphur and other compounds like HCl. Process steam required in the gasifier is generated internally using the high temperature flue gases leaving the combustor. For the methanation plant, the steam is generated using flue gas exiting from the gasifier. A part of this heat is also utilised in a steam cycle for producing electric power from a steam turbine. In order to produce synthetic natural gas from SNG, syngas is first processed for optimising the H<sub>2</sub>/CO ratio in a high temperature water gas shift reactor. Methanation plant consists of three methanation reactors in series. At the end of methanation process, the feed gas is rich in carbon dioxide and steam. Selexol process is used for removing carbon dioxide. Finally, the water is condensed out and the feed gas is compressed to 200 bar at 25 °C. The calculations mentioned so far were performed using Aspen Plus. The efficiency of fuel production was 59.7%.

The next part of the study was made using Cycle-Tempo, wherein a hybrid power production plant using solid oxide fuel cells and gas turbine was setup. Take off conditions were used as design conditions for determining the size of the system. Sensitivity analysis was performed for the operating pressure of the hybrid system. A 3<sup>rd</sup> generation anode supported cell made by Delphi was used. The operating current density at design point was 5000 A/m<sup>2</sup>. Off –design calculations were made for assessing the system performance during cruise conditions. Also two configurations for the air-preheater were analysed. The optimal system performance was achieved with the air preheater placed between two gas turbine units which is denoted by configuration B in the study. The exergetic efficiency of this system was 69.6%. The total well to efficiency was then calculated to be 41.6 %. A comparison with earlier study utilizing liquid H<sub>2</sub> for powering a similar hybrid system resulted in a well to wheel efficiency of 11.3%. The endurance of the proposed aircraft concept with compressed SNG as fuel is 2.31 days which is significantly lesser than the endurance of

## Future Work

The study reveals many avenues of further action. It has already been mentioned that this study is part of a larger, more comprehensive study of analysing different fuel options for powering an unmanned aerial vehicle. Liquid hydrogen has already been studied as a fuel option.

•*Energy density*: SNG storage tanks weigh more than the SNG they carry. In the current study, fuel tanks contribute to more than 55% of the fuel and tank storage system. It is hard to predict advancements in storage technology that will lead to significant reductions in this mass fraction. A different approach would be to consider liquefied fuels. Methanol, for example, could be generated using Fischer-Tropsch synthesis which would have a higher energy density than compressed SNG. Also, fuels like DME can be compressed more easily to increase the volumetric density.

•*Greenhouse gas emissions*. The main focus of the study was to analyse the hybrid system performance thermodynamically. This meant that the study of greenhouse gas emissions was largely restricted by choice. In order to develop a truly feasible system, the policy measures of in the near future need to be taken into account. The general policy trend favours reduction in GHG emissions. However, it should be pointed out that reduction in GHG emissions would cost reduction in thermodynamic performance of the system. This is much evident in the comparison for LH<sub>2</sub> and compressed SNG fuel options.

•*Power consumption in gasification plant*: For the production of compressed SNG from biomass, gasification plant consumes power on a net basis. This presents problem in defining exergy efficiency of the gasification plant. In future, it should be possible to produce this power in situ. A fraction of the product SNG stream can be used in a SOFC to produce this power. Then it will be possible to achieve a a more realistic value of the exergy efficiency of SNG production process.

•*Source of biomass*: The source of biomass in this study was virgin birch wood. Gasification of biomass is a novel technology indeed but there are plenty of other sources which can be utilised. Waste streams from agricultural waste, municipal sewage waste can also be utilised for producing fuels. However, the gasification technology would vary greatly mainly because of the

composition of biomass.

•*Aircraft system*: The present study utilizes the aircraft concept proposed by NASA in 2007. This concept was optimised for a design based on proton exchange membrane fuel cell. Although, the design of this aircraft system was completely out of the scope of the current study, design modifications to better match the use of a SOFC-GT hybrid system could possibly make a difference for its endurance.

•*Gas turbine inlet temperatures*: Gas turbines with higher inlet temperatures theoretically will have higher efficiencies for a given stack exhaust temperature. The turbine inlet temperatures could be further manipulated by changing the position of air and fuel preheaters and much evidence has been found in the current study.

•*Intermediate temperature SOFCs*: Research on solid oxide fuel cells is largely focussed on reducing the material costs and reducing the operating temperature of the fuel cell provides one of the solutions. With the use of bi electrode supported cells and metal supported cells much higher power densities are achievable. However, the operating current density for such cells needs to be further investigated.

\

---

## Reflections

The scale on which this study was conducted was indeed large and, frankly, does not defy expectation. Just like a large puzzle that one has never solved before, it was difficult to imagine how the final picture would look like. Although previous well to wheel studies were available, they failed to deliver sufficient insight into system sizing. Regrettably, the system sizing aspect of the study had to be fast forwarded considering the time limitations in the project. The author therefore makes but one suggestion for aspiring engineers, who wish to take this study further. It would be very helpful to develop a thorough understanding of the well to wheels analysis concept and plan the process chain before starting the analysis. During the course of this analysis it becomes possible to take the study in many different directions. A good plan can thus help in, the very least, preserving the sanity of the analyst in question.

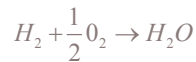
As a final remark, the project provided a very clear picture of how the fuel cell technology would be making progress in the near future. During the course

of this project, the author was able to critically compare the developments in field of fuel cell technology for aircrafts, comprehend the know-how needed to implement similar systems for land based applications such as automobiles, onsite power generation, distributed power generation and combined power and heating applications. The vastness of the fields of application has become a source of inspiration that the author will carry forward into the future. The learning outcomes are immensely helpful to the author who hopes to graduate with a master of science degree with the culmination of this project.

# Appendix 1

## Thermodynamics of Solid oxide fuel cells - An Introduction

This text serves the purpose of a quick primer for the thermodynamic operation of a solid oxide fuel cell (SOFC). SOFC converts the chemical energy stored in a molecule to electrical energy or work. However, the chemical energy stored within a molecule is not entirely available for producing work. It is a good point to start off by estimating how much chemical energy is actually available for conversion. In this case, it becomes extremely relevant to talk in terms of gibbs free energy of formation. Standard gibbs free energy of formation,  $\Delta_f g^0$  for different species can be calculated using standard values of constituting elements in reference state. Using heats of reaction and equilibrium measurements these calculations can be carried out. For example, the cell reaction for a SOFC is:

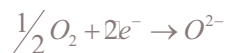


The gibbs free energy of formation for the individual molecules,  $\Delta_f g^0$  is available from standard tables. Using these values, the gibbs free energy of reaction can be calculated as :

$$\Delta_{rxn} g^0 = \Delta_f g_{H_2O}^0 - \Delta_f g_{H_2}^0 - \frac{1}{2} \Delta_f g_{O_2}^0$$

Where,  $\Delta_{rxn} g^0$  is the amount of work that is available for conversion in the SOFC.

The overall cell reactions can be broken down into half-cell reactions. This gives an idea about the number of electron taking part in the cell reactions. The half-cell reactions taking place are:



As can be seen, the number of electrons taking part per mole of reacting fuel ( $H_2$ ) is 2. According to Faradays law of electrolysis, the electrical charge,  $Q$ , that can flow in an external circuit is given by:

$$Q = nZe$$

Where  $n$  is the number of electron in the circuit, the  $Z$  is the Avogadro's constant and  $e$  is the charge of an electron. In the equation above, the product of  $Z$  and  $e$  is known as Faraday's constant. The electrical work that can be derived is therefore

$$W = Q.E$$

Where  $E$  is the voltage in the external circuit. For a reversible SOFC, this work should be equal to the gibbs free energy of the reaction. Then the reversible or the open circuit voltage for the SOFC can be written as

$$E^0 = \frac{\Delta_{rxn} g^0}{-2F}$$

For a chemical reaction, the actual cell potential depends on the activity of the reaction components.

Activity is defined as the ratio of fugacity of the species in a mixture to its standard fugacity (Sandler, 2006). For an ideal gas,  $i$ , in a mixture, this equation is reduced to the following form:

$$a_i = \frac{P_i}{P_i^0}$$

Where  $P_i^0$  is the standard pressure of the gas. The actual cell potential is given by the Nernst equation (Sandler, 2006):

$$-nFE = -nFE^0 + RT \ln \prod a_i$$

For the SOFC, this equation can be rewritten for the hydrogen reaction as,

$$E = E^0 + \frac{RT}{nF} \ln \left( \frac{\frac{P_{H_2}}{P^0} \left( \frac{P_{O_2}}{P^0} \right)^{1/2}}{\frac{P_{H_2O}}{P^0}}} \right)$$

Or at a standard pressure of 1 atm, the equation becomes simply,

$$E = E^0 + \frac{RT}{nF} \ln \left( \frac{P_{H_2} P_{O_2}^{1/2}}{P_{H_2O}} \right)$$

This equation describes the dependence of the cell potential on the partial pressure of the reacting species. It is now possible to understand how the cell potential might change depending on the extent of specie consumption in the SOFC. From the inlet to the outlet the specie are consumed in the reaction and therefore the local cell potential changes. However, the cell is designed to operate at a relatively constant voltage, therefore this change is reflected in the current density.

So far, equations describing a reversible cell have been mentioned. As hardly any process is reversible, the actual operating voltage of the fuel cell is different from the open circuit voltage. Figure below shows the polarisation curve for a SOFC operating methane free biogas (composed mainly of CO and H<sub>2</sub>). In the figure, the open circuit voltage is around 0.9 V and with increasing current density the operating voltage decreases. These voltage drops are associated with increasing irreversibility encountered due to high operating current densities. There are several avenues for irreversibility in a SOFC and they have been adequately documented (Larminie et al, 2003). The net operating voltage is obtained as follows

$$V = E - \sum \Delta V_{loss}$$

The major losses can be accounted for by the following phenomenon:

- Activation losses: At the surface of the electrodes the half-cell reactions are taking place continuously in both the forward and reverse directions. However, at equilibrium no net current is produced because the rates of forward and backward reactions are similar. The current here is called exchange current and in order to get a high exchange current density, this equilibrium needs to be shifted in the forward direction. This can be done by increasing the operating temperature, increasing the catalytic activity on the surface by using high concentration of the reactant or increasing the surface area. The loss activation overpotential can be modelled using the Butler- Vollermer equation:

$$\Delta V_{act} = A \ln \left( \frac{i}{i_0} \right)$$

Where,  $i_0$  is the exchange current density and  $i$  is current density (A/m<sup>2</sup>).

- Fuel crossover and internal currents: There is always the possibility that some amount of fuel passes through the electrolyte and combines with the oxidant and thereby giving rise to an internal current. This decreases the cell potential. This effect highly pronounced in low temperature fuel cells, but with increasing operating temperature, the internal currents are reduced and the drop in cell potential

is also reduced. The voltage drop can be modelled by modifying the Butler-Vollmer equation:

$$\Delta V = A \ln \left( \frac{i + i_{int}}{i_0} \right)$$

\Where,  $i_{int}$  is the internal current density

•Ohmic losses: Resistance to flow of ions in the electrolyte and electrons in the electrode are categorised as ohmic losses. These losses depend on the thickness of the electrolyte and the conductivity of the electrodes. A thinner electrolyte and a more conductive electrode would have lower ohmic losses than normal. The ohmic losses are modelled as follows:

$$\Delta V_{ohm} = ir$$

Where  $r$  is area specific resistance ( $\Omega.m^2$ ).

•Mass transportation losses: Across the length of the fuel cell, the fuel and oxidant get consumed and consequently there is a drop in the partial pressure. This results in the voltage drop. There could be many reasons for drop in partial pressure: non uniformity of the porous structure of the electrode, internal reformation reactions, carbon deposition on the catalyst – these all contribute to decreased mass flow of the fuel for the fuel cell reaction and therefore increases the overvoltage. The following equation can be used for modelling mass transport losses:

$$\Delta V_m = m \exp(ni)$$

Where  $m$  and  $n$  are constants (Larminie et al.,2003).

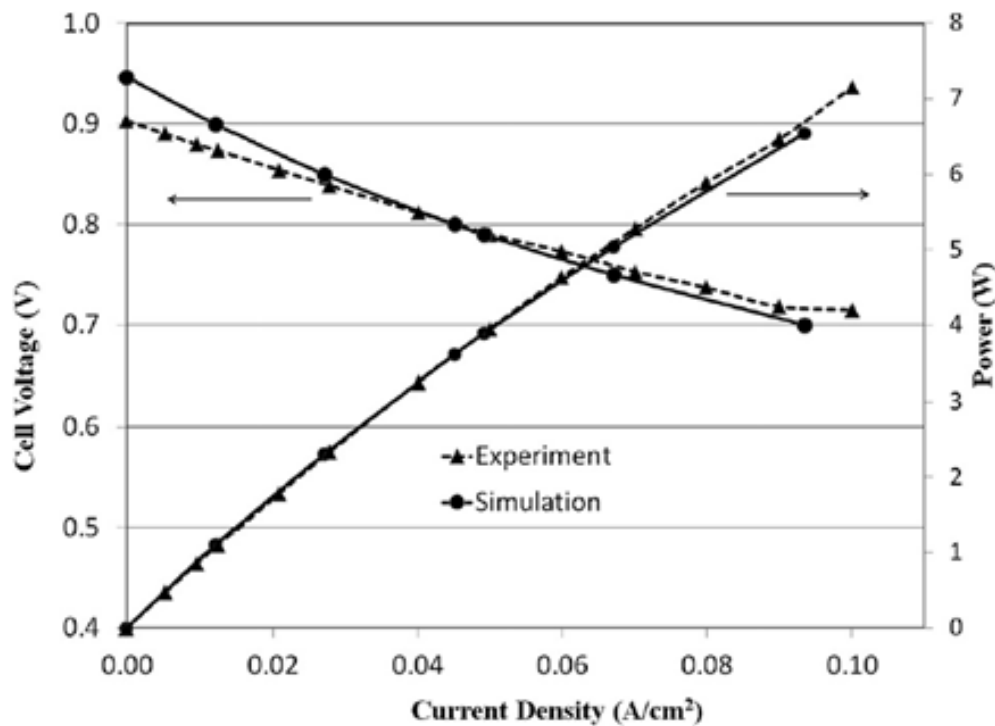


Figure. POLARISATION CURVE FOR SOFC OPERATING ON METHANE FREE BIOGAS. SOURCE (RAZBANI ET AL., 2013)

---

## *References*

Larminie, James, Andrew Dicks, and Maurice S. McDonald. Fuel cell systems explained. Vol. 2. New York: Wiley, 2003.

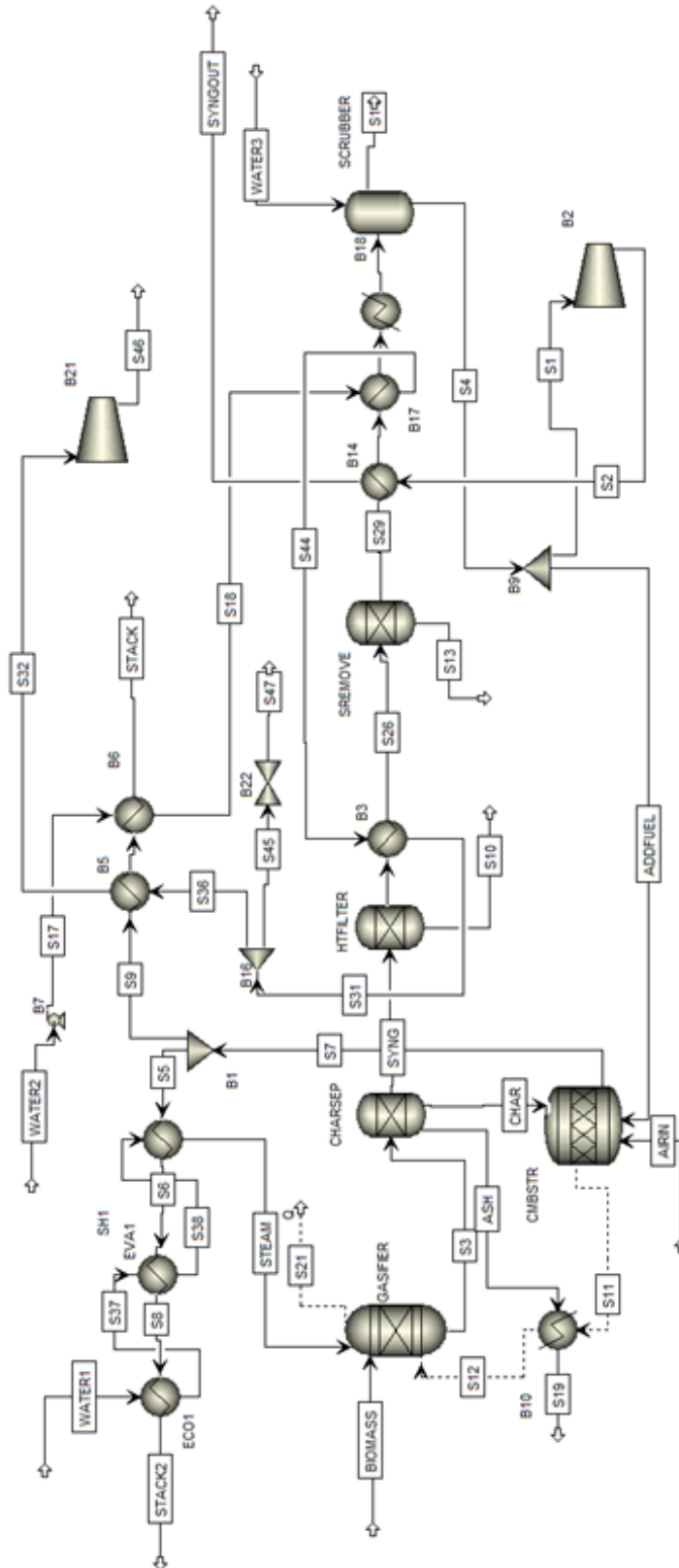
Razbani, Omid, Mohsen Assadi, and Martin Andersson. "Three dimensional CFD modeling and experimental validation of an electrolyte supported solid oxide fuel cell fed with methane-free biogas." *International Journal of Hydrogen Energy* 38.24 (2013): 10068-10080.

Sandler, Stanley I. Chemical, biochemical, and engineering thermodynamics. Vol. 4. Hoboken, NJ: John Wiley & Sons, 2006.



# Appendix 4A

## Gasification plant scheme



# Appendix 4B

## Atomic balance calculations for gasifier

Input specifications for atomic balance

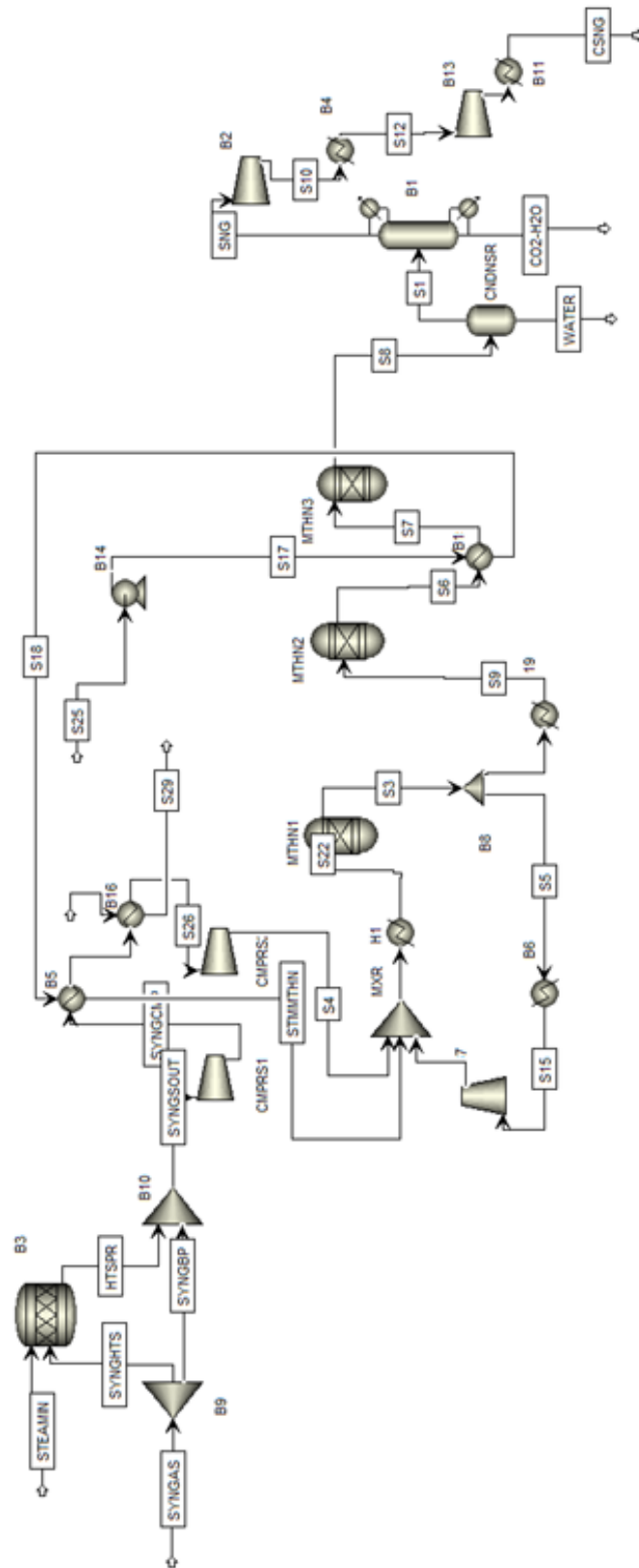
<i>Input Specifications</i>	<i>Value</i>	<i>units</i>
input power	50	MW
LHV	16,07	MJ/kg
Mass flow rate	3,111	kg/s
carbon conversion	87%	
S/C ratio	0,63	
Gas yield	1,037	kg/kg
Char composition	35,2	g/Nm <sup>3</sup>
C	0,83	kg/kg
H	0,03	kg/kg
O	0,14	kg/kg

Output composition on mole basis from the gasifer.

<i>Output</i>	<i>mol%</i>
H <sub>2</sub>	43,9%
CO	26,2%
CO <sub>2</sub>	17,7%
CH <sub>4</sub>	9,4%
C <sub>2</sub> H <sub>4</sub>	2,5%
C <sub>2</sub> H <sub>6</sub>	0,3%
HC (C <sub>3</sub> -C <sub>5</sub> ) (mol%)	0,1%

# Appendix 4C

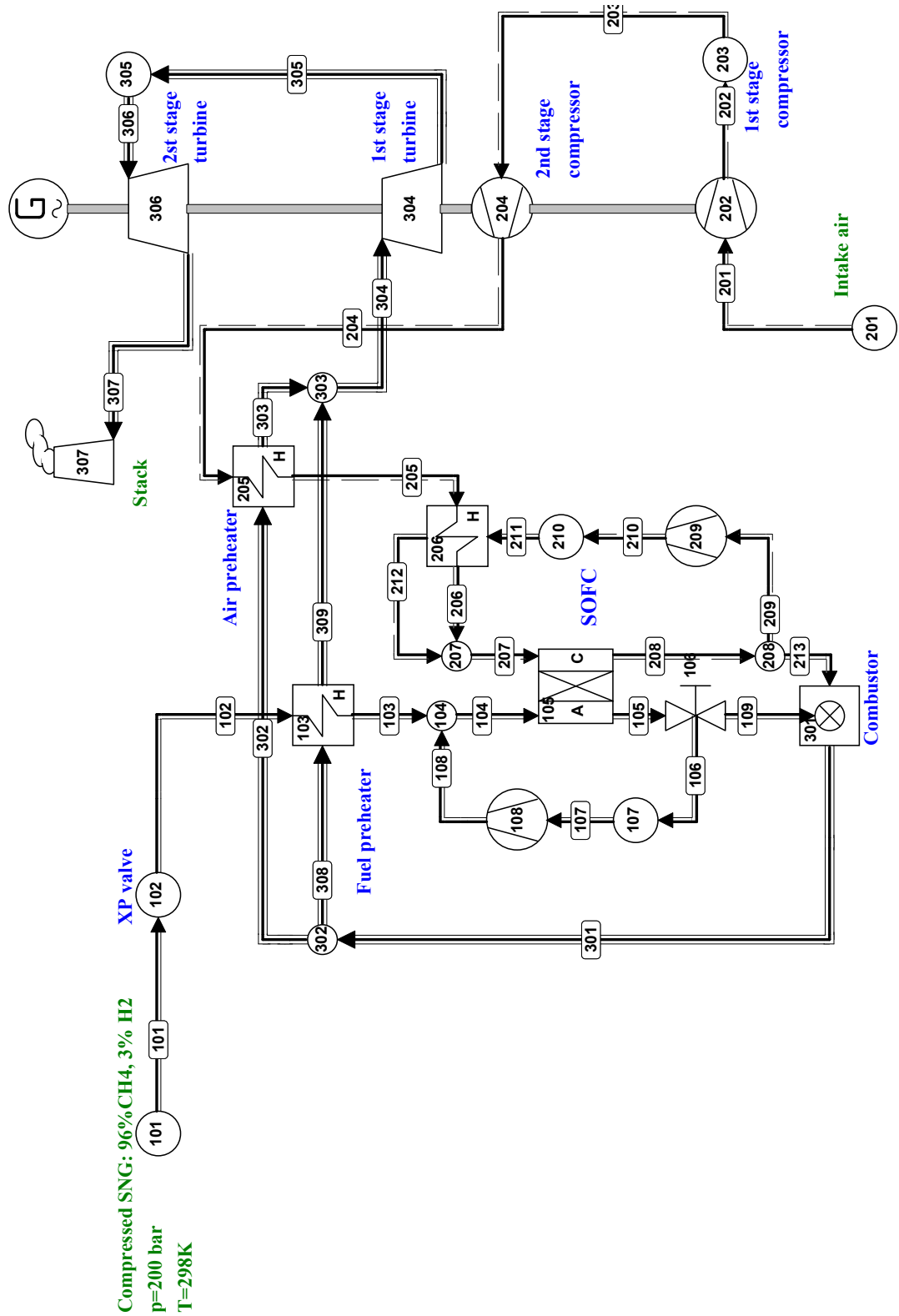
## Methanation plant scheme



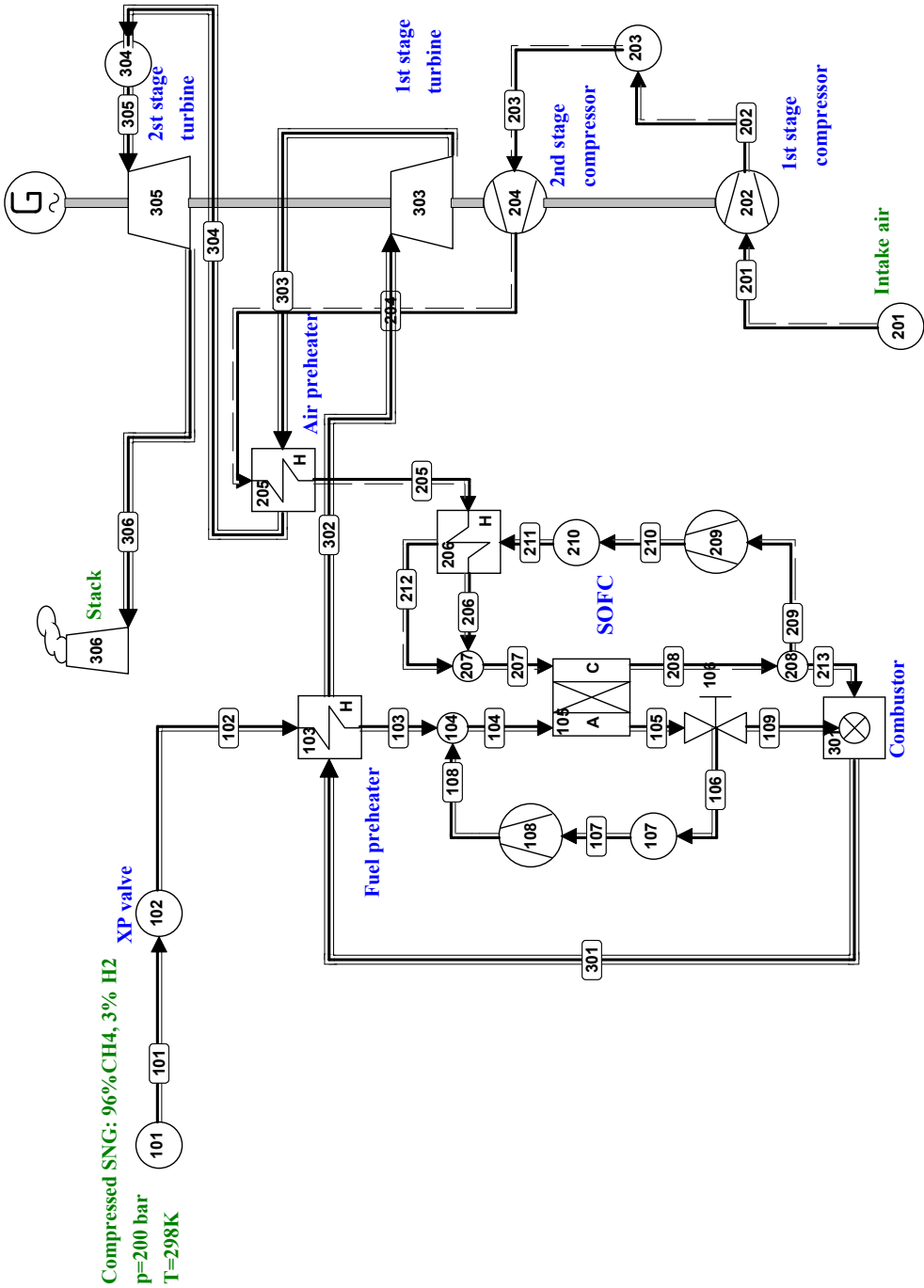
# Appendix 4D

## SOFC-GT system flowsheet in Cycle Tempo

Air preheater configuration A



Air preheater configuration B



# Appendix 4E

## System sizing requirements for aircraft concepts

Mass requirements of the aircraft

<b>Component</b>	<b>Mass limit (kg)</b>
Fuel Cell/Electric motor drive	1138
Engine mount	194
Propeller	93
Fuel Systems	264
Fuel	1150
Total mass of propulsive unit	2839
Remaining mass of the aircraft (including structure)	2083
Total mass at take-off	4922

Output composition on mole basis from the gasifier.

<b>Parameter</b>	<b>Value</b>	<b>Unit</b>
Lift to Drag ratio ( Cl/CD)	38	
Lift Coefficient (Cl)	0.75	
Propeller Efficiency	80.00	%
Wing area	260	m <sup>2</sup>
Cruising power	100	kW

# Appendix 5A *Gasification unit outlet gas composition*

	<b>Composition (molar %)</b>	<b>Flow rate(kg/hr)</b>	<b>Temperature (°C)</b>	<b>Pressure (bar)</b>
Gasifier Output		14988,1	850	1,3
	CH <sub>4</sub> 7.69%			
	CO 19.63%			
	CO <sub>2</sub> 11.80%			
	H <sub>2</sub> 26.28%			
	H <sub>2</sub> O 32.61%			
	C <sub>2</sub> H <sub>4</sub> 1.35%			
	C <sub>2</sub> H <sub>6</sub> 0.61%			
	NH <sub>3</sub> 0.03%			
	Ash	32.64489	920	1.3
Flue gas		22495.25	920	1.3
	Ar 0.83%			
	CO <sub>2</sub> 14.97%			
	H <sub>2</sub> O 11.72%			
	NH <sub>3</sub> 0.00%			
	O <sub>2</sub> 2.97%			
	N <sub>2</sub> 69.52%			
Gas Cleaning Output		9076.204	350	1.3
	CH <sub>4</sub> 10.53%			
	CO 26.87%			
	CO <sub>2</sub> 16.16%			
	H <sub>2</sub> 35.97%			
	H <sub>2</sub> O 7.80%			
	C <sub>2</sub> H <sub>4</sub> 1.85%			
	C <sub>2</sub> H <sub>6</sub> 0.82%			
	NH <sub>3</sub> 0.01%			
Shift reaction		11328.2	440.5	1.3
	CH <sub>4</sub> 8.32%			
	CO 12.07%			
	CO <sub>2</sub> 21.96%			
	H <sub>2</sub> 37.62%			
	H <sub>2</sub> O 17.92%			
	C <sub>2</sub> H <sub>4</sub> 1.46%			

Methanation	C <sub>2</sub> H <sub>6</sub>	0.65%	14571	300	16.5
	CH <sub>4</sub>	22.53%			
	CO	0.01%			
	CO <sub>2</sub>	21.39%			
	H <sub>2</sub>	0.72%			
	H <sub>2</sub> O	55.35%			
	C <sub>2</sub> H <sub>4</sub>	0.00%			
C <sub>2</sub> H <sub>6</sub>	0.00%				
Compressed SNG	CH <sub>4</sub>	95.89%	2336.51	25	200
	CO	0.03%			
	CO <sub>2</sub>	0.92%			
	H <sub>2</sub>	3.10%			
	H <sub>2</sub> O	0.06%			



# Appendix 5B

## Air composition at 21 km altitude

Using the formulae described in Chapter 3, the atmospheric temperature and pressure at this altitude can be calculated as  $-56.5\text{ }^{\circ}\text{C}$  and  $.046752\text{ bar}$  respectively. The water pressure at this altitude can be calculated from Clausius Clapeyron equation.

<b>Component</b>	<b>Mole fraction</b>
	0.93
CO <sub>2</sub>	0.03
N <sub>2</sub>	78.08
O <sub>2</sub>	20.95
Moisture	0.07

# Appendix 5C *Air composition at 21 km altitude*

Exergy destruction during take-off ( Design condition)

	<b>T1.5A</b>	<b>T1.5B</b>	<b>T5A</b>	<b>T5B</b>
GT1	0.726	0.748	1.037	2.083
GT2			1.377	1.221
Comb	10.454	11.243	8.772	10.175
FC	15.469	15.214	12.783	12.705
HEX103	2.393	2.530	2.158	2.011
HEX207	0.307	12.556	0.240	4.444
HEX206	13.334	0.307	5.323	0.251
Comp 210	0.398	0.399	0.098	0.103
Comp202	0.975	0.982	1.380	1.175
Comp108	0.017	0.015	0.006	0.006
Comp204			1.412	1.747
Node 104	1.201	1.155	1.004	1.110
Node 208	0.233	0.208	0.282	0.226
XPValve	3.154	3.112	2.117	2.110
Stack	41.930	39.283	29.345	27.350
Exergy in	210.910	209.872	187.965	187.265
Work	120.138	120.301	120.621	120.731
Stack	41.930	24.905	29.345	27.350
Destroyed	48.660	64.660	37.989	39.179
Balance	0.182	0.006	0.010	0.005
Exergy efficiency	57.0%	57.3%	64.2%	64.5%

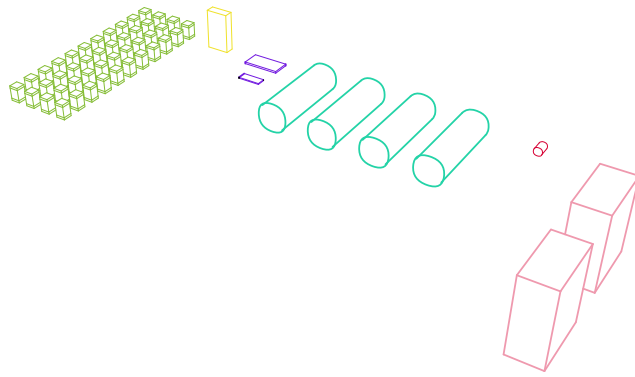
Exergy destruction during cruise ( off-design condition)

	<b>C1.5A</b>	<b>C1.5B</b>	<b>C5A</b>	<b>C5B</b>
GT1	0.707	0.672	0.733	0.728
GT2	0.713	0.707	0.745	0.776
Comb	2.511	2.534	2.632	2.640
FC	1.622	1.012	1.717	1.848
HEX103	0.623	0.651	0.612	0.651
HEX 206-207	0.149	0.176	0.153	0.119
HEX205	0.659	0.311	0.675	0.413
Comp 202	0.693	0.691	0.719	0.755
Comp 205	0.742	0.740	0.769	0.755
Comp 108	0.009	0.007	0.009	0.032
Comp 210	0.016	0.020	-0.008	0.552
XP valve	0.777	0.768	0.786	0.768
Stack	10.048	9.363	10.094	9.127
Gen	3.251	3.274	3.249	3.256
Node104	0.072	0.332	0.560	0.055

---

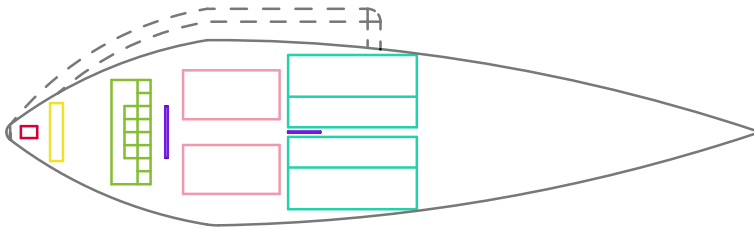
Exergy in	72.579	71.754	73.404	71.754
Work	50.042	50.335	50.030	49.946
Stack	10.048	9.363	10.094	9.127
Destroyed	12.528	11.895	13.333	13.347
Balance	-0.038	0.160	-0.054	-0.667
Exergy efficiency	68.9%	70.1%	68.2%	69.6%

# Appendix 5d *System sizing - Volumetric sizing*

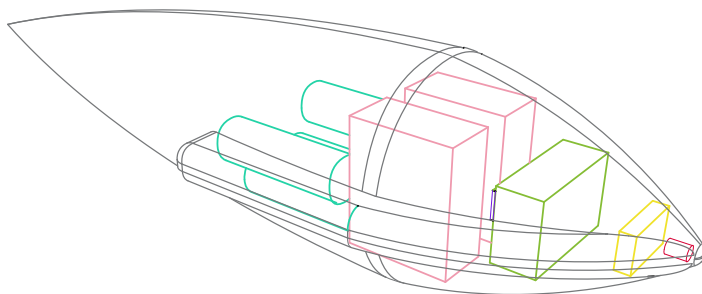


- Electric Motor
- Inverter
- Heat exchangers
- SOFC Stacks
- Nacelle
- Turbochargers
- CNG Cylinders



Individual components



Side view



Isometric view



Process & Energy  
Building 39, Leeghwaterstraat  
Delft , 2628 CA  
E: [hardikjoshi24@gmail.com](mailto:hardikjoshi24@gmail.com)